

Drivers and impacts of Eastern African rainfall variability

Paul I. Palmer^{1,2}✉, Caroline M. Wainwright^{3,18}, Bo Dong^{4,5}, Ross I. Maidment⁴, Kevin G. Wheeler⁶, Nicola Gedney⁷, Jonathan E. Hickman^{8,9}, Nima Madani^{10,11}, Sonja S. Folwell¹², Gamal Abdo¹³, Richard P. Allan^{4,5}, Emily C. L. Black⁴, Liang Feng^{1,2}, Masilin Gudoshava¹⁴, Keith Haines^{4,5}, Chris Huntingford¹², Mary Kilavi¹⁵, Mark F. Lunt¹, Ahmed Shaaban^{16,17} & Andrew G. Turner⁴

Abstract

Eastern Africa exhibits bimodal rainfall consisting of long rains (March–May) and short rains (October–December), changes in which have profound socioeconomic and environmental impacts. In this Review, we examine the drivers and corresponding impacts of Eastern African rainfall variability. Remote teleconnections, namely the El Niño–Southern Oscillation and the Indian Ocean Dipole, exert a dominant influence on interannual variability. From the mid-1980s to 2010, the long rains have tended toward a drier state (trends of -0.65 to -2.95 mm season⁻¹ year⁻¹), with some recovery thereafter, while the short rains have become wetter since the mid 1980s (1.44 to 2.36 mm season⁻¹ year⁻¹). These trends, overlain by substantial year-to-year variations, affect the severity and frequency of extreme flooding and droughts, the stability of food and energy systems, the susceptibility to water-borne and vector-borne diseases, and ecosystem stability. Climate model projections of rainfall changes differ, but there is some consensus that the short rains will deliver more rainfall than the long rains by 2030–2040, with implications for sustaining agricultural yields and triggering climate-related public health emergencies. Mitigating the impacts of future Eastern African climate requires continued investments in agriculture, clean water, medical and emergency infrastructures, and development and adoption of adaptation strategies, as well as targeted early-warning systems driven by improved meteorological observations.

Sections

Introduction

Drivers of rainfall variability

Observed changes in Eastern African rainfall

Impacts of observed rainfall variations

Future changes

Summary and future perspectives

Introduction

Seasonal rainfall is integral to the 457 million people living across Eastern Africa, a region including Burundi, Djibouti, Eritrea, Ethiopia, Kenya, Rwanda, Somalia, South Sudan, Sudan, Tanzania and Uganda (Box 1). The number, duration and timing of these rainfall seasons varies, driven principally by the movement of the intertropical convergence zone (ITCZ)¹. For instance, the most northerly and southerly regions (northern Ethiopia, Eritrea, Sudan, South Sudan and southern Tanzania) experience a single summer wet season for their respective hemispheres. In contrast, countries between these latitudinal extremes (encompassing Kenya, Uganda, Somalia, Burundi, Rwanda and parts of northern Tanzania and southern Ethiopia) experience two wet seasons. These two wet seasons occur during boreal spring (typically March–May, MAM; the more intense long rains) and autumn (typically October–December, OND; the less intense short rains), although there are substantial regional variations in these timings.

This seasonal rainfall is vital to the health and economic prosperity of the region. For example, long rains support agricultural production and thus national food security. Rain-fed agriculture, in turn, has a substantial role in the economy of many Eastern African countries. Agriculture employs 67% of people in Ethiopia, 80% in Somalia, 54% in Kenya, 63% in Eritrea and 38% in Sudan². Agriculture also represents an extensive contribution to the annual multibillion-dollar export of goods such as sugar, tea, coffee, tobacco, nuts and seeds, cut flowers and vegetables³. Moreover, rainfall is pivotal to energy production, particularly given that hydropower represents a large fraction of electricity generation in Eastern Africa⁴. Aquifer recharge from rainfall^{5,6} also provides a sustainable reservoir of groundwater for potable water (and irrigation) during periods of drought⁵, demonstrating the importance of rainfall for water security, especially when looking to the future⁷.

Observed rainfall variability, particularly disruption to the long and short rains, can therefore result in a wide range of humanitarian, economic and environmental impacts. For example, three anomalously low rain seasons over Somalia from April 2016 to December 2017 resulted in sustained and widespread drought conditions that led to considerable losses of agricultural crops and livestock⁸. Consequently, more than six million people faced acute food shortages and malnutrition⁹, exacerbated by a shortage of potable water that led to disease outbreak. A similar situation unfolded in 2022 (refs. ^{10,11}) following poor rain seasons since late 2020. In stark contrast, consecutive anomalously high rain seasons over South Sudan since 2019 led to prolonged flooding, directly affecting more than 900,000 people¹² each year. Recurrent flooding further damaged water treatment facilities, leaving millions without potable water and resulting in the outbreak of water-borne diseases¹². Moreover, fields that typically support subsistence farming are submerged by floodwater, reducing the land available for cultivation, and so affecting crop yields¹³ and livestock productivity¹⁴. To help to mitigate such impacts and inform future adaptation changes, it is therefore vital to fully understand all aspects of Eastern African rainfall, particularly in light of continued changes arising from anthropogenic warming¹⁵.

In this Review, we evaluate the key drivers of Eastern African rainfall variability, the consequent societal impacts and how they are likely to change with future climate. We begin by outlining observed rainfall variability and the corresponding physical drivers over Eastern Africa, focusing on regions with a bimodal rainfall season. We subsequently outline the economic, humanitarian and environmental impacts of such observed rainfall variability. Next, we describe the major climatological changes anticipated over the region and the associated likely

future impacts. Finally, we identify key gaps in knowledge and how these can be addressed in future research.

Drivers of rainfall variability

The timing and magnitude of the seasonal cycle of rainfall vary across Eastern Africa (Fig. 1). A single peaked seasonal cycle is evident over most of the Nile basin during June–August (Fig. 1a), whereas two distinct rainfall seasons (short rains and long rains) are observed over the Juba–Shabelle (Fig. 1b) and northeast coast basins (Fig. 1c). Some combination of the two occurs over the Rift Valley basin (Fig. 1d) and the central-east coast basin (Fig. 1e).

In each of these basins, there are substantial seasonal and interannual variations in rainfall totals (Fig. 1). For example, the standard deviation over the Nile basin during August (typically the wettest month) is 17 mm month⁻¹, representing -12% of the long-term monthly mean. The Juba–Shabelle basin, by contrast, exhibits much larger variability. Specifically, the standard deviation reaches 36 mm month⁻¹ and 52 mm month⁻¹ during the peaks of the long rains (April) and short rains (October), respectively, representing 30% and 60% of their long-term means. Such variability has meant that short rains totals between 1983 and 2019 have ranged between a minimum of 34 mm month⁻¹ in 2003 (39% of the long-term mean) and a maximum of 305 mm month⁻¹ in 1997 (355% of the long-term mean). This variability is driven by various local and remote physical processes, which are now discussed.

Global teleconnections

Rainfall variability over Eastern Africa is influenced by several modes of climate variability (Fig. 2), including the El Niño–Southern Oscillation (ENSO), the Indian Ocean Dipole (IOD), the Quasi-Biennial Oscillation (QBO) and the Madden–Julian Oscillation (MJO).

The IOD is a key driver of such interannual rainfall variability, describing differences in sea surface temperature (SST) anomaly between the western (50° E to 70° E, 10° S to 10° N) and eastern (90° E to 110° E, 10° S to 0° S) Indian Ocean. The positive IOD (signifying an SST anomaly difference of at least +0.4 °C for at least three months between the warmer west and cooler east) is linked with wetter short rains over Eastern Africa (Fig. 2a). During such phases, precipitation totals can be 2–3 times the long-term mean¹⁶, as seen in 1997, 2006, 2012, 2015 and 2019. In contrast, the negative IOD (defined by a sustained negative SST difference of at least 0.4 °C) is associated with weaker short rains¹⁷, resulting in 20–60% of the long-term mean rainfall, as evident during 1996, 1998, 2010 and 2016 (Fig. 2b).

ENSO, which describes SST variability in the central and eastern tropical Pacific, is also connected to changes in the short rains¹⁸. El Niño conditions, associated with warmer SST anomalies over the central and eastern Pacific, typically result in wetter short rains, whereas La Niña conditions, associated with cooler SST anomalies, result in drier short rains¹⁹ (Fig. 2). ENSO's impact on Eastern Africa is, however, strongly mediated by the IOD¹⁸. The typical concurrence of positive IOD with East Pacific El Niño, and negative IOD with East Pacific La Niña, act to amplify precipitation responses. For instance, the coincidence of the 1997 El Niño with a strong positive IOD event led to short rain anomalies twice the climatological mean¹⁶. In contrast, the strong central Pacific El Niño of 2015 coincided with a weaker IOD, producing anomalies -50% above the climatological mean¹⁸. However, these relationships are nonlinear, as demonstrated by extreme 2019/2020 rainfall that occurred during an anomalously positive phase of the IOD but neutral ENSO conditions²⁰.

The IOD and ENSO physically influence Eastern African short rains by modifying regional atmospheric circulation features (Fig. 2a,b).

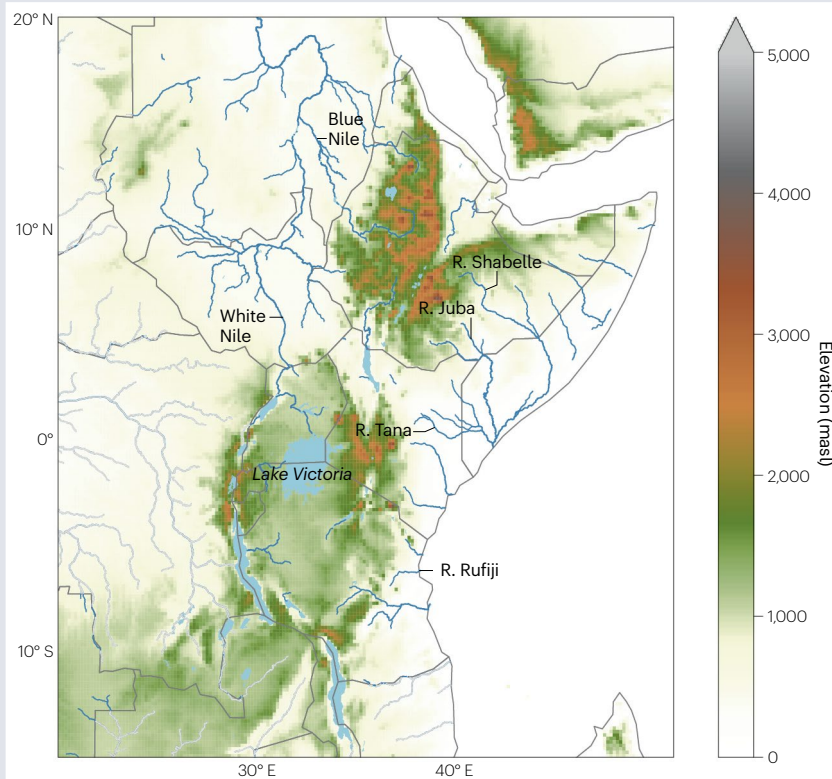
Box 1

Physical geography of Eastern Africa

The physical geography of Eastern Africa is relevant to the dynamics of rainfall weather systems^{49,234} and to the subsequent surface movement of water (see figure). The region is dominated by the East African Rift, running from the Afar Triple Junction near the Red Sea southwards through Eastern Africa to Mozambique, which also produced the Ethiopian and Kenyan highlands.

Eastern Africa is dominated by the Nile River basin but also encompasses tributaries of the Congo as well several regionally important rivers draining eastwards into the Red Sea, the Gulf of Aden and the Indian Ocean. Two endorheic rivers, the Awash and Omo, terminate in the Afar depression and Lake Turkana, respectively. The Nile basin contains several Rift Valley lakes, including Lake Victoria, which collects water from Burundi, Rwanda, northern Tanzania and the Kenyan Highlands, and has an important role in regulating flows in the White Nile downstream.

Tributaries draining the western Ethiopian highlands bring additional seasonal flows (during August–October), with the largest of these, the Blue Nile, joining at Khartoum to form the main River Nile²³⁵. Lake Kivu and Lake Tanganyika and its tributaries in western Tanzania form the headwaters of the Congo²³⁶. Watersheds east and south of the Ethiopian highlands and eastern Rift Valley flow into the Indian Ocean, providing an essential source of water to populations in more arid coastal plains, for example Shabelle and Juba in Somalia. In addition to the Rift Valley lakes, areas



of extensive seasonal flooding, for example the Sudd in South Sudan, lead to considerable water losses to the atmosphere by evaporation²³⁷.

Specifically, positive IOD and El Niño conditions weaken the Indian Ocean Walker circulation^{21,22}; positive SST anomalies over the western Indian Ocean drive a strong rising branch of the Walker circulation, and negative SST anomalies over Southeast Asia an anomalous sinking branch of the Walker circulation, opposite to climatological conditions. A sinking branch of the Walker circulation over the eastern Indian Ocean, in turn, favours a rising branch over Eastern Africa associated with elevated rainfall. During concurrent positive IOD and El Niño events, these dynamical responses are amplified, enhancing short rain anomalies¹⁸.

ENSO also influences long rains. Strong El Niño events can be followed by cool La Niña conditions in the East Pacific that coincide with warmer SSTs in the western Pacific (sometimes referred to as a 'Western V' pattern²³). Warmer SSTs in the western equatorial Pacific are linked to drier short rains, and warmer SSTs in the western North Pacific are associated with dry conditions during the long rains. Warmer SSTs over the western North Pacific strengthen the Walker circulation that suppresses long rains. This SST pattern led to successive dry seasons and droughts during 2016–2017 (ref. ²³). Variations in the long rains

are less sensitive to changes in IOD²⁴, because the IOD peaks several months later (during September–November) than the peak in the long rains.

The MJO – which describes the eastward propagation of enhanced regional convection across the tropics – is an additional driver of sub-seasonal rainfall variability over Eastern Africa, influencing both the long and short rains on a monthly basis²⁵. MJO phases 2–4 are linked with large-scale convection in the Indian Ocean, resulting in westerly wind anomalies and enhanced rainfall¹⁸ over the Eastern African highlands^{26–28} (Box 1). This relationship is strongest in November, December, March and May, but tends to be weaker during October and April, owing to seasonal changes in dynamic and thermodynamic mechanisms associated with large-scale atmospheric circulation and localized dynamics²⁹. In contrast, MJO phases 6–8 are associated with suppressed convection across Eastern Africa and the western Indian Ocean, but wet conditions over low-lying coastal regions^{26,28}. Greater seasonal rainfall accumulations are observed during a long rains season when the MJO is more active in any phase³⁰, with the MJO explaining ~20% of the observed interannual rainfall variations.

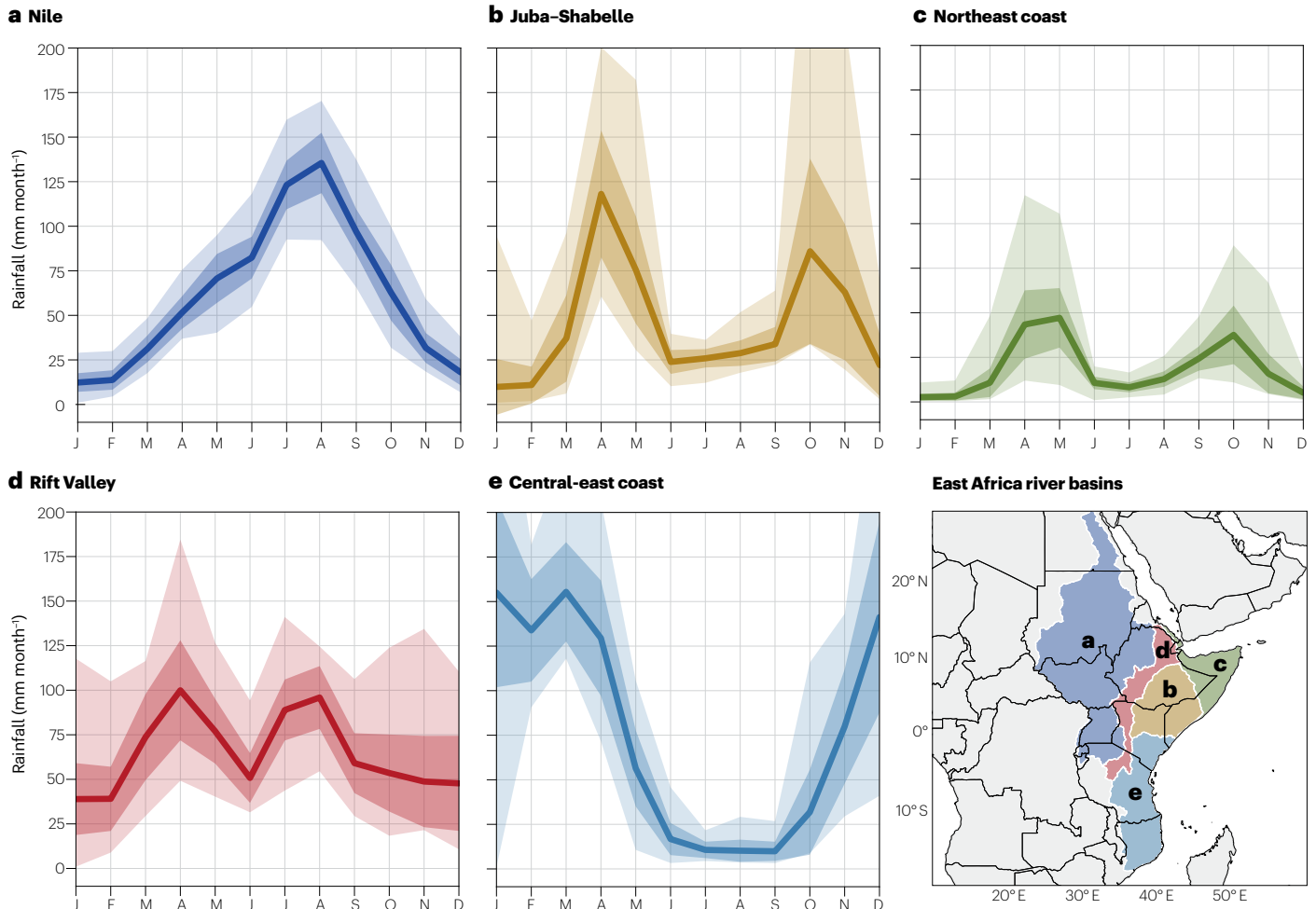


Fig. 1 | Seasonal cycle of rainfall. **a**, Area-averaged mean seasonal rainfall in the Nile basin (area **a** in the map, as delineated by HydroBASINS²²⁹) from 1983 to 2019. The dark envelope denotes the standard deviation about the monthly mean values and the light envelope the range of values. Values are calculated from monthly gridded gauge data from the Global Precipitation Climatology Centre (GPCC)^{230,231}. **b**, As in panel **a**, but for the Juba–Shabelle basin (area **b** in the map). **c**, As in panel **a**, but for the northeast coast basin (area **c** in the map). **d**, As in panel **a**, but for the Rift Valley basin (area **d** in the map). **e**, As in panel **a**, but for the central-east coast basin (area **e** in the map). Substantial differences in the magnitude, variation and (bimodal) seasonal cycle of rainfall are evident across Eastern Africa.

Through its relationship with the MJO³¹, the eastward phase of the QBO also influences Eastern African rainfall. Above-average long rains are linked to an easterly QBO in the preceding September–November³⁰. This six-month lag³² is consistent with the timescale associated with the descent of mid-stratospheric wind anomalies to the tropopause³³. The QBO typically explains <20% of observed interannual rainfall variations, and the strength of this lagged correlation is dependent on which model reanalysis is used³⁴, owing to model-specific assumptions about convective parameterizations.

Local drivers

In addition to global teleconnections, local drivers also exert a prominent influence of rainfall variability over Eastern Africa by imposing higher-order SST variations on the Indian Ocean. For instance, local variations in Indian Ocean SSTs, particularly those in the west that are partially controlled by the IOD³⁰, are also linked with variability in both rainy seasons. Here, warmer SSTs heat the boundary layer, drive

anomalous ascent that enhances rainfall, opposing the climatological subsidence and corresponding drying typical for the region. Positive SST anomalies in the western Indian Ocean increase the magnitude of short rains over 95% of equatorial Eastern Africa³⁵, and explain 9–26% of observed rainfall variations during the long rains³⁰. The positive correlation between western Indian Ocean SSTs and rainfall is strongest at the beginning and end of the long rains season³⁶ when the rainfall is less well established and more susceptible to local and remote forcing. Rainfall during the peak of the long rains (April) is also significantly correlated with southern Atlantic SSTs, whereby cooler SSTs lead to higher rain rates over Kenya driven by zonal winds over central Africa³⁶.

Tropical cyclones are also an important contributor to rainfall variability over parts of Eastern Africa. For instance, the presence of tropical cyclones in the southwest Indian Ocean (when the MJO is in phases 3–4) is associated with low-level westerly anomalies over Eastern Africa that enhance rainfall³⁷. This rain-bearing westerly flow is more likely when the cyclones are located to the east of Madagascar rather

than the west²⁷. Indeed, Cyclones Dumazile and Eliakim in 2018, located east of Madagascar, were associated with westerly flow, enhancing rainfall by -100 mm across eastern Tanzania, most of Kenya, and parts of Uganda, South Sudan, southern Ethiopia and western Somalia. In contrast, Cyclone Idai in 2019 was located west of Madagascar and coincided with a drier period, some 50–100 mm below average across most of northern Tanzania and central/southern Kenya^{37,38}.

The influence of the Congo airmass, characterized by 700-hPa zonal winds, has also been associated with interannual variability of the long rains^{27,36} (Fig. 2a). Despite climatological easterly winds, westerly winds originating from the Congo sometimes occur during March–May (often linked to phase 3–4 of the MJO²⁷), bringing moist air that leads to convergence around Lake Victoria and enhances rainfall^{27,36}. Indeed, the cumulative rainfall total of the long rains is further strongly correlated with 700-hPa zonal winds across the Congo basin and Gulf of Guinea. Furthermore, enhanced surface westerlies from the Congo basin, driven by a higher geopotential height gradient over the Congo basin than the western Indian Ocean, lead to wetter long rains over Tanzania³⁹.

Observed changes in Eastern African rainfall

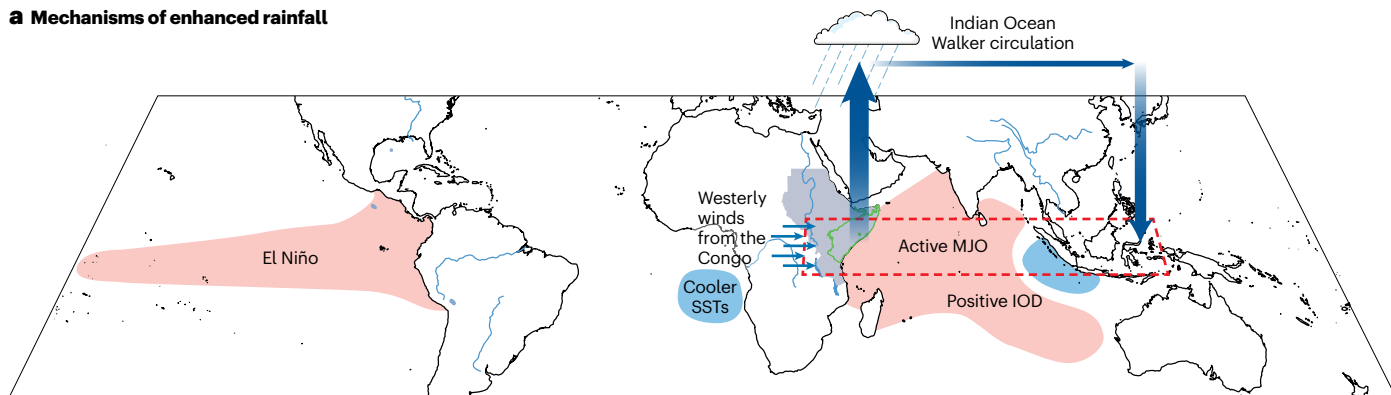
In addition to interannual variability driven by remote and local drivers, precipitation also shows decadal-scale trends across Eastern Africa. A range of satellite-derived rainfall data products have helped to quantify these changes since the early 1980s^{40,41} (Fig. 3). However, the magnitude

and sign of the rainfall trends derived from individual satellite datasets are inconsistent, with the largest discrepancies in the eastern Congo basin and the greatest consistency in the Ethiopian highlands (Fig. 3a,b). Moreover, substantial differences between satellite products and gauge-based records add to the uncertainty^{42–44} (Fig. 3c,d). Areal-weighted rainfall, however, offers better agreement across datasets (Fig. 3c,d), particularly after 2000 when there are fewer gaps in the satellite records⁴⁵, resulting in greater confidence in long and short rains trends, as are now discussed.

Long rains

The long rains exhibit considerable decadal as well as year-to-year variability. In particular, consistent negative trends are observed from 1985 to 2010 over Eastern Africa (Fig. 3, boxed region), the magnitude of which varies from -0.65 to -2.95 mm season⁻¹ year⁻¹ depending on the dataset used (Fig. 3c). Notable declines occurred in -1999 and 2010–2011 (refs. 46–49). Trends calculated up until -2017 also continue to be negative. However, very wet long rains in 2018 and 2020 indicate some recovery (Fig. 3a,c), with trends computed between 1983 and 2021 no longer indicating widespread and consistent drying. Instead, less consistency emerges among datasets (Fig. 3a,c). For example, over 1983–2019, TAMSAT indicates a general wetting trend of 1.41 mm season⁻¹ yr⁻¹ (0.52% season⁻¹ yr⁻¹), whereas the Global Precipitation Climatology Centre (GPCC) dataset indicates an overall drying trend of -0.12 mm season⁻¹ yr⁻¹ (-0.03% season⁻¹ yr⁻¹).

a Mechanisms of enhanced rainfall



b Mechanisms of reduced rainfall

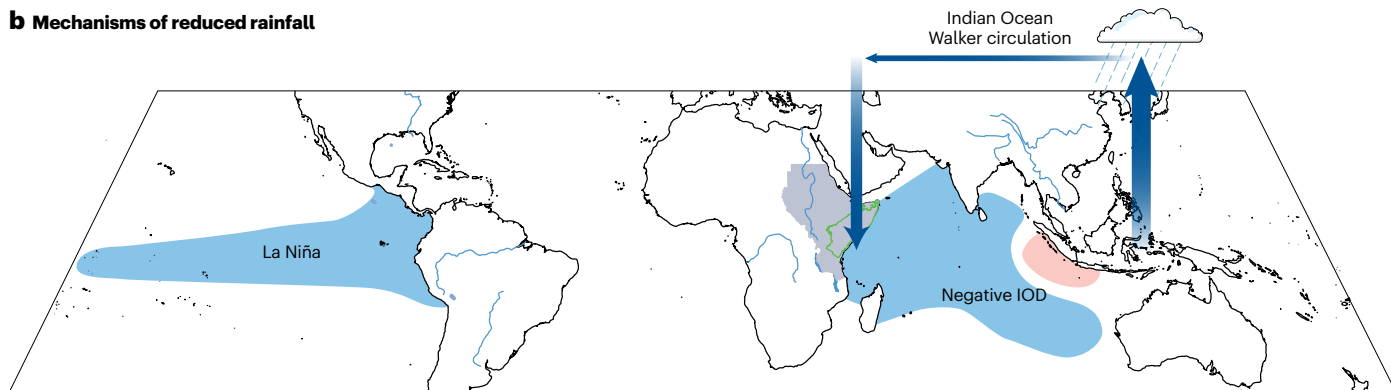
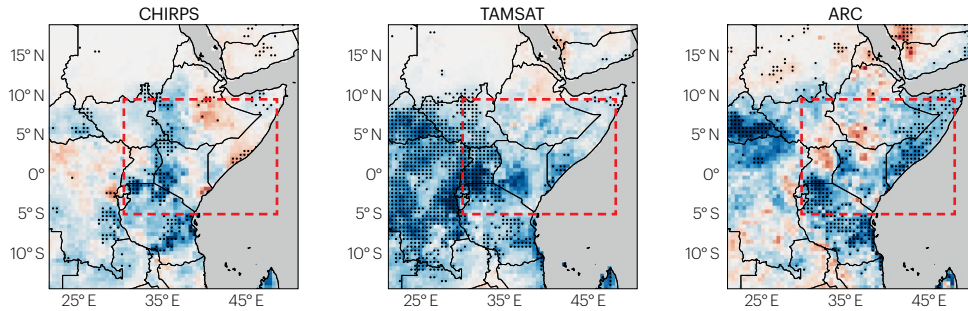


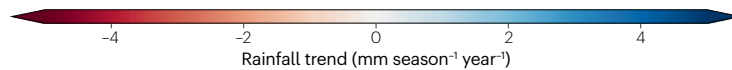
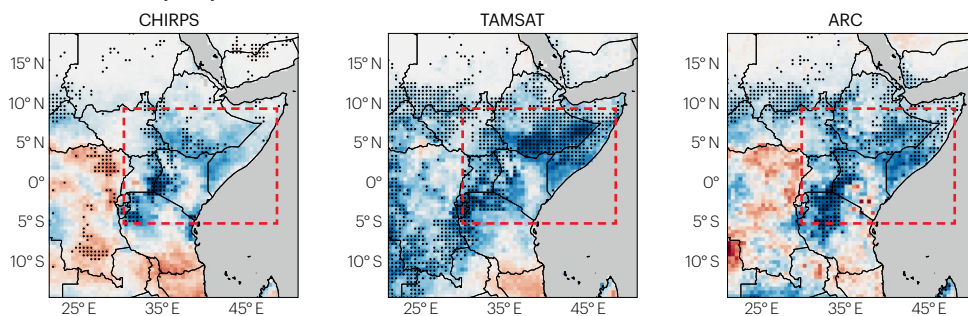
Fig. 2 | Physical processes influencing rainfall variability. **a**, Teleconnection mechanisms that lead to enhanced rainfall over Eastern Africa (marked by grey shading). The green contour marks the region within Eastern Africa that experiences two wet seasons per year. Orange and blue shading represent

warm and cool sea surface temperatures (SSTs), respectively. **b**, As in **a**, but for mechanisms that lead to reduced rainfall over Eastern Africa. Rainfall variations are determined by processes that act on local spatial scales and via atmospheric teleconnections. IOD, Indian Ocean Dipole; MJO, Madden–Julian Oscillation.

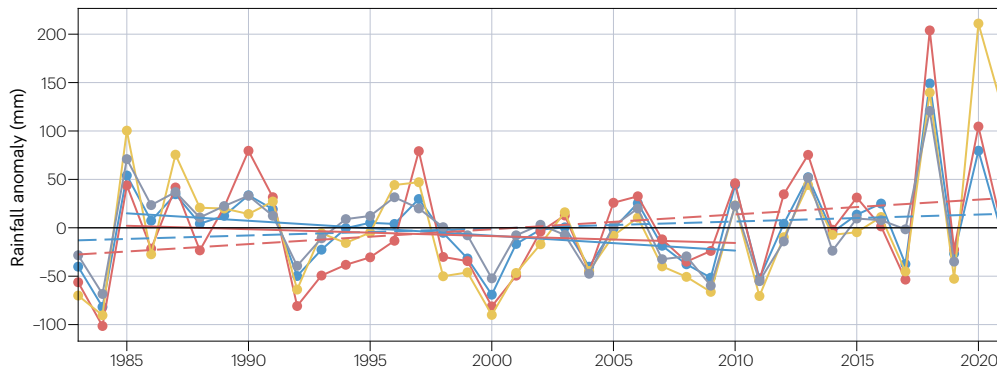
a Long rains trend (MAM)



b Short rains trend (OND)



c Spatially averaged long rains (MAM)



d Spatially averaged short rains (OND)

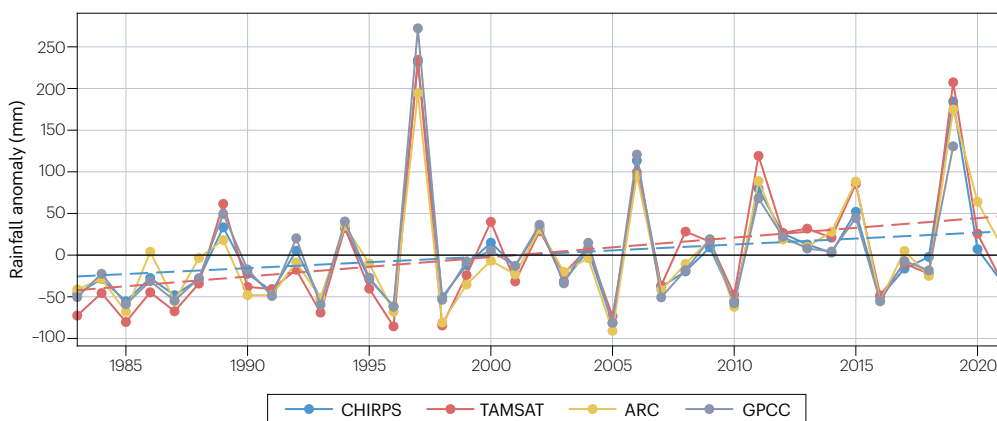


Fig. 3 | Spatial and temporal rainfall variability. **a**, Mean rainfall trends during the long rains (March–May: MAM) over 1983–2021 for three datasets: CHIRPS²³² (top left); TAMSAT⁴⁰ (top middle); and ARC⁸⁸ (top right). Stippling denotes statistically significant trends at the 95% confidence level using the Wald test. **b**, As in panel **a**, but for the short rains (October–December: OND). **c**, Area-weighted total rainfall anomalies during MAM over part of Eastern Africa

(30–50° E, 5° S to 10° N; red boxes in **a** and **b**) for the CHIRPS, TAMSAT, ARC and GPCP^{25,255} datasets. Anomalies are calculated relative to the 1983–2021 monthly means. Dashed and solid lines denote linear trends over 1983–2021 and 1985–2010, respectively, for CHIRPS (blue) and TAMSAT (red). **d**, As in panel **c**, but for OND. There is better agreement between positive trends (1.44–2.36 mm season⁻¹ year⁻¹) determined by different rainfall data products for the short rains.

The reduction in long rains up to the 2010s has been linked to Pacific Ocean SST variability^{50–52}. For instance, positive SST anomalies in the Western V pattern (encapsulating the western Pacific warm pool and tongues extending northeastward toward Hawaii and southeastward into the southern central Pacific^{23,53}) enhance convection over the western equatorial Pacific, create an anomalous Walker circulation over the Indian Ocean, strengthen the upper-level easterlies, increase subsidence over Eastern Africa, and consequently reduce rainfall during the long rains^{46,54}. In some instances, the strengthening of the upper-level easterlies has been highlighted as the dominant driver in this process, with minimal connections to Walker circulation variability⁵⁴. Furthermore, rapid warming of the West Pacific relative to the East Pacific since 1998, associated with a negative phase of the Pacific Decadal Oscillation⁵⁵, has been linked with greater susceptibility of the long rains to drought during La Niña events, increasing the risk of concurrent short and long rain droughts²³. Strengthening of the west minus east SST gradient across the Pacific since 1998 has also led to a stronger Walker circulation and faster Pacific trade winds^{56,57}, resulting in drying over Eastern Africa via Indian Ocean teleconnection, in contrast to a weaker SST gradient and associated Walker circulation simulated by coupled climate models⁵⁸.

Other factors have also been proposed to explain the observed decline in the long rains. Most notably, the rainfall reduction has been linked to a shortening of the long rains season⁴⁷ (that is, a later onset and earlier cessation) from the 1980s to late 2000s. This shortening is related to faster SST warming in the Arabian Sea compared with further south, enhancing the pressure gradient and resulting in a faster-moving rainband. Declining westerly 700-hPa winds are also linked with the decadal drying trend during the long rains⁴⁸, driven by changes in geopotential height gradient that are associated with increased heating around Arabia and the Sahara⁴⁸. Finally, internal variability^{47,48}, such as variations in SST that are not linked with radiative forcing, is also thought to be a driver.

Short rains

In contrast to longer-term drying trend of the long rains, a consistent wetting trend is apparent for the short rains over 1983–2021 (Fig. 3b,d) over Eastern Africa (Fig. 3a, boxed region). Over this time period, trends range from 1.44 to 2.36 mm season⁻¹ yr⁻¹ (0.85–1.49% season⁻¹ yr⁻¹), highlighting an increase in short rain totals of 50–100 mm over the study period. These values are broadly consistent across each dataset. Spatially, all datasets exhibit this increasing rainfall trend over large parts of Tanzania, Uganda, Kenya, Somalia and Ethiopia (Fig. 3b).

As with the long rains, these regional-mean long-term linear trends are punctuated with periods of pronounced anomalous rainfall, including 1997–1998 and 2019–2020 when short rains totals were 2–3 times higher than climatological values¹⁶. Indeed, rainfall anomalies of 100–250 mm year⁻¹ are observed in 1997, 2006, 2012, 2015 and 2019, linked to variability associated with ENSO and corresponding interactions with the IOD^{49,51,52,59}. Such short-term variability, driven by changes in ENSO and the IOD, and unequal warming across the Indian Ocean⁶⁰

(the western Indian Ocean SST index has increased by 0.48 °C while the eastern index has increased by only 0.26 °C, 1979–2012) are the primary drivers of the regional-mean wetting during the short rains.

Anthropogenic connections

Large year-to-year variability in the long and short rains makes it difficult to isolate an anthropogenic imprint to any changes in Eastern African rainfall variability. Palaeoclimate reconstructions provide a longer-term view of rainfall changes over Eastern Africa. They show that changes in rainfall in the past century across the globe are not unprecedented in the context of the past two millennia, but the rate at which rainfall is changing is unusual. These data reveal a drying trend over the past two centuries⁵⁰ and an increase in drought frequency over the Horn of Africa during March–May⁶¹.

Greenhouse-gas-induced warming drives an increase in atmospheric moisture and its convergence, intensifying wet seasons, while higher temperatures and greater evaporative demand intensify dry seasons, contributing to a greater severity of wet and dry extremes⁶². Cooling from anthropogenic aerosols has partially offset these greenhouse gas changes, and, through an additional altered global distribution of aerosol forcing, has been implicated in a southward shift in the African ITCZ from the 1950s to the 1980s⁶³. Recovery from this altered state has been attributed to a combination of greenhouse gas and aerosol forcing⁶⁴. Although there is some consensus about the human influence on rainfall over Eastern Africa (via greenhouse-gas-induced warming and cooling from anthropogenic aerosols^{21,64,65}), the anthropogenic influence on the physical processes (specifically the IOD) that control year-to-year rainfall changes is less clear^{54,66}. Based on a combined model and data analysis, drought trends over Eastern Africa are most consistent with changes in precipitation rather than increasing temperature⁶⁷.

An increased frequency of the positive phase of the IOD during the second half of the twentieth century has not led to higher seasonal rainfall amounts compared with the first half of the twentieth century⁵⁴. This observation is consistent with understanding of how a warming climate perturbs the thermal structure of the atmosphere and the circulation of the tropical oceans^{68,69}, resulting in a long-term weakening of Walker and Hadley circulations and the narrowing of the ITCZ^{54,70,71}. Yet observed strengthening of the Walker circulation since the 1990s, associated with rapid warming of the tropical west Pacific relative to the east Pacific, is not reproduced by simulations and linked with systematic model biases that might limit the projections of Eastern African rainfall⁵⁸. Therefore, anthropogenic signals of Eastern Africa rainfall are yet to be clearly established in the observational record, and the future projections assessed below should be interpreted in the context of these complex present-day drivers and uncertainties.

Impacts of observed rainfall variations

Local and remotely driven variability in the short and long rains has substantial and multifarious environmental, humanitarian and economic impacts, including those on agriculture, natural ecosystems,

water security and human health, as are now discussed. These impacts are not exhaustive but represent a diverse subset of widely researched topics and demonstrate the complex and evolving challenges faced by Eastern African countries. Note that precipitation impacts do not occur in isolation and often coincide with changes in temperature that can reinforce^{72–74} or weaken⁷⁵ impacts, complicating explicit attribution.

Agricultural impacts

Rainfall variability across Eastern Africa affects agriculture directly and indirectly. Much agriculture in the region is rain-fed. As such, failure of seasonal rains result in agricultural droughts, the frequency of which has increased from once every ten years in the early 1900s to once every three years since 2005 (ref. ⁷⁶). Although small- and large-scale irrigation schemes are helping to mitigate the impacts^{77,78}, minimal infrastructure exists to retain, redistribute and store water to cope with this intra-seasonal and interannual variability. The resulting loss of agricultural production has thus been the cause of some of the most well-known humanitarian disasters in the twentieth and twenty-first centuries, including the 1974 Sahel and 1984 Ethiopia/Sudan droughts which resulted in an estimated 325,000 and 450,000 deaths, respectively^{79–81}.

Other examples include three major droughts over Somalia (2011/2012, 2016/2017 and 2021/2022), and the historic droughts in Ethiopia^{82,83} during 2015 and 1997/1998. For example, although the 1997/1998 drought over northern Ethiopia was not as extreme or as widespread as that of 1984, cereal production⁸⁴ declined by 25% during this period, resulting in price increases of 15–45%. This surge in price was due to drought-related declines in crop yields, as well as reductions in cultivated land from malnourished oxen⁸⁵. Reduced crops also caused cattle mortality rates of 26% in some regions from dehydration, starvation and disease⁸⁶. Drought early-warning systems^{87,88} have sought (and arguably helped) to mitigate deaths associated with food security^{89,90} by enhancing rapid humanitarian responses from governments and international aid. ENSO is one contributing factor driving hydrological extremes and corresponding agricultural impacts over Eastern Africa. However, ENSO's impacts in this area are spatially variable⁹¹, with El Niño events driving lower than normal rainfall over northern Ethiopia but higher than normal rainfall over southern Ethiopia that can lead to flooding.

Indeed, although below-normal rainfall threatens agriculture, so does an increase in rainfall intensity. In regions that are moisture-limited, benefits from increased rainfall can be expected⁹². In regions with low-permeability soils such as the clay vertisols of the subhumid regions of Ethiopia that have infiltration capacities of only 2.5 to 6.0 cm per day, however, the landscape can be easily overwhelmed by intensive rainfall⁹³. Low permeability of irrigated lands results in waterlogging and crop damage, and poor drainage systems substantially limit the production potential of the soils⁹⁴. For example, productivity losses of 45% over 60 years have been recorded for some Ethiopian sugar plantations owing to waterlogging. Furthermore, agricultural topsoil is eroded when runoff from sloped terrain exceeds the rate of soil intake⁹⁵, affecting future productivity. Unusually heavy rainfall over northern Ethiopia during March and April 2016, immediately following extensive drought conditions, for instance, led to widespread flooding, landslides, displacement of people and damage to crops.

Such flooding also influences the population and movement of desert locusts (*Schistocerca gregaria*)^{96–99}, a key threat to agricultural crops. Heavy and extensive rainfall provides moist soil for egg laying, and the subsequent rain-fed flush of vegetation provides shelter and food for the locusts, leading to widespread damage by locust plagues.

For example, 114,000, 41,000 and 36,000 hectares of sorghum, maize and wheat, respectively, were estimated to be damaged¹⁰⁰ in Ethiopia between December 2019 and March 2020, linked to the worst locust outbreak in 25 years for the country. Moreover, an estimated US\$8.5 billion in crop damage occurred in Yemen and Eastern Africa during 2020, amplifying threats to food security¹⁰¹. Crop damage during these and other (1986/1987 and 1992/1993) years is linked to a positive IOD and the corresponding enhanced rainfall¹⁰². However, these remote drivers often interact with local drivers, which in the case of the 2020 outbreaks includes the rare landfall of two tropical cyclones in the Arabian Peninsula during 2018, exponential growth in breeding through the creation of ephemeral lakes, their southward migration to Eastern Africa, and subsequent establishment of the swarm from IOD-related enhanced vegetation growth. The COVID-19 pandemic, along with other factors, prevented proactive interventions.

Ecosystem impacts

Rainfall variability also has strong bearing on various ecosystem functions, including terrestrial gross primary production (GPP), wildfire activity and wetland emissions of greenhouse gases.

Water availability exerts a considerable influence on Eastern Africa's terrestrial GPP¹⁰³ – the total amount of carbon fixed by plants. On a regional basis, tropical forest and savannah ecosystems are typically limited more by water than by sunlight^{104,105}. Interannual variations in water availability¹⁰³ associated with rainfall and groundwater are thus highly correlated with GPP, resulting in GPP variations of $\pm 10\%$ of climatological values (the mean being $-3.08 \pm 0.19 \text{ Pg yr}^{-1}$); for forest ecosystems, these correlations drop when rainfall exceeds 1,800 mm, perhaps owing to reduced sunlight from cloud cover¹⁰³. Groundwater reservoirs are particularly important in this regard, acting as a temporary buffer against drought during years of low rainfall for sufficiently deep rooting systems, but only if they have an opportunity to replenish during anomalously wet years. Satellite data demonstrate these connections¹⁰⁶. For instance, during 2005, which marks a time preceded by years of anomalously low rainfall and depleted groundwater, a 5% drop (-0.15 Pg yr^{-1}) in GPP was observed over the region that encompasses Somalia and eastern Ethiopia. In contrast, 2015 was marked by similarly low rainfall, but five consecutive high-rainfall years replenished groundwater reserves to produce GPP close to the climatological mean (3.19 Pg yr^{-1}). Similarly, a strong El Niño in 2010 saw widespread increases in rainfall, resulting in GPP increases of -5% ($+0.15 \text{ Pg yr}^{-1}$).

By influencing GPP, rainfall variability can also influence vegetation fire activity and consequently emissions of air pollutants, CO₂ and other greenhouse gases (GHGs)^{107–109}. For example, above-average rainfall during the growing season increases plant productivity, thereby increasing the fuel load available for burning in subsequent seasons or years¹¹⁰. In contrast, above-average rainfall during the dry season can suppress fire activity, although fire ignition via lightning is enhanced during moist convection¹¹¹. Both processes have proven to be important in Eastern Africa¹¹². Indeed, over 2001–2012, changes in rainfall explained about 20% of the negative trends in burned area in South Sudan¹¹³. Some of this variability can, in turn, be linked to ENSO, with El Niño years typically causing a small reduction in burned area anomalies in forest and non-forest ecosystems over northern hemispheric Africa. Generally, however, ENSO has a smaller role in burned area than in other tropical biomass burning regions^{114,115}.

Tropical wetland emissions of methane^{116,117} and ammonia^{118,119} (NH₃) are further related to long and short rain variability over Eastern Africa via relationships with inundation extent, water table depth and

soil moisture. Aquatic production of methane, for instance, arises from anoxic decomposition of organic matter from root systems and decaying plants. Changes in wetland extent and associated vegetation flushing, particularly over South Sudan and Ethiopia, thereby have had a strong influence on global methane atmospheric growth rates^{120–123}. Indeed, wetland emissions from the Sudd in South Sudan during 2010–2016 represented about a third of the global atmospheric growth of methane. Rainfall anomalies arising from a strong positive IOD during 2018–2019 further caused higher methane emissions, explaining a quarter of the global atmospheric methane growth rate for that year¹²¹. The anomalous global atmospheric methane growth rates in 2020 (refs. 124,125) and 2021 (ref. 125) have also been partly attributed to anomalous Eastern African wetland emissions.

Ammonia, abiotically volatilized from ammonium in soils, is also influenced by soil moisture. When soils with high moisture content start to dry out, NH_3 -nitrogen tends to become more concentrated at the same time as there are reduced limits on gas diffusion through soils, which, along with other factors, leads to enhanced NH_3 emissions^{126–128}. These processes produce a large seasonal increase in NH_3 concentrations (8×10^{15} to 13×10^{15} molecules cm^{-2}) over salt flats in Tanzania as the waters of Lake Natron, a soda lake with relatively alkaline pH, recede during the dry season¹²⁹. A similar seasonal behaviour has been observed over the Sudd wetlands in South Sudan¹³⁰. Roughly half of the Sudd wetlands are permanently flooded, with part of the remaining wetland area drying each year¹³¹ to various extents. For example, NH_3 concentrations over the region reached nearly 30×10^{15} molecules cm^{-2} in 2010 when seasonal drying of the Sudd was most extensive, compared with 11×10^{15} molecules cm^{-2} in 2014 when drying was least extensive¹³⁰.

Water and energy security

Rainfall variability has direct consequences for human wellbeing, including generation of clean energy from hydropower, transboundary water management and urban infrastructure.

Hydropower development is often seen as a viable solution to meet growing energy demands in Eastern Africa. Indeed, current hydropower capacity contributes about 50% of electrical generation in East Africa Power Pool (Burundi, Djibouti, DRC, Egypt, Ethiopia, Kenya, Libya, Rwanda, Somalia, South Sudan, Sudan, Tanzania, and Uganda) countries, with a planned doubling by 2030, mostly in the Nile basin. However, a strong dependency on hydropower places the entire economic system at the mercy of variable hydrological conditions¹³², especially in an increasingly uncertain climatic future^{133,134}. Although Zambia is not part of Eastern Africa, it serves as an example of the multiplicative consequences of rainfall variations on hydropower, particularly regarding the Kariba Dam, the provider of 1,830 megawatts of hydroelectric power to Zambia and Zimbabwe. Extremely dry conditions during 2015/2016, linked with a strong El Niño, reduced inflow into Lake Kariba, dropping lake levels to 12% of capacity in January 2016, just above the minimum necessary to generate electricity¹³⁵. This drop led to a major energy deficit in Zambia, causing daily power outages, particularly affecting Lusaka Province and the Copper Belt, that were only resolved by buying energy from neighbouring countries. As a result of these outages (and a reduction in global copper price) in the Copper Belt, an estimated 19% drop in GDP occurred¹³⁶. Conversely, excess rain, as in March 2010, affected the discharge rates of downstream dams, leading to major floods that affected hundreds of thousands of people.

More generally, variability in precipitation presents an important issue for regional water security and conflict security in Eastern African

countries that include transboundary rivers¹³⁷. For example, construction of the Grand Ethiopian Renaissance Dam (GERD) on the Blue Nile River has the potential to be the biggest risk of conflict between neighbouring Eastern African countries¹³⁸. The dam is part of Ethiopia's economic growth plan to become Africa's largest hydropower exporter. However, there is concern that GERD will reduce downstream water for irrigation and drinking, and to a lesser extent reduce hydropower capacity. Years of heavy rainfall over Ethiopia, such as 2020, can help fill the GERD and result in release of sufficient water to Sudan and Egypt¹³⁹. Proponents of GERD argue that in years with lower rainfall, the dam's water storage can be used to alleviate drought in downstream countries. Diplomatic negotiations are ongoing, but the situation serves as an example of the complexities associated with transboundary water. So far, only minor conflicts have been observed, primarily led by herders and farmers in neighbouring countries fighting over pasture and water for livestock. Safely handling severe flooding and drought events requires close communication between managers of different dams, some of which will be across political borders, to avoid harm to co-riparian nations¹³⁸ and to avert international conflict¹⁴⁰.

Rainfall fluctuations, particularly heavy rain, also have considerable impact on infrastructure. Periods of intense rainfall can quickly overwhelm inadequate infrastructure¹⁴¹, resulting in overflowing drainage systems, flooded houses and suspension of sewage treatment that often leads to a range of health emergencies¹⁴². Flooding can also damage roads and railways built with limited budgets and inadequate engineering, disrupting the transportation of workers and food supplies from rural to urban areas and consequently affecting economic activity¹⁴³. For example, heavy rainfall over Sudan in 2020 led to extensive flooding that damaged or destroyed 112,000 homes, causing a three-month state of emergency¹⁴⁴. Similarly, heavy rains and flash flooding in 2021 affected 88,000 people in 13 out of 18 Sudanese states, with widespread damage and destruction of houses and clean water sources. Flash flooding also affected the sewage systems of camps for internally displaced persons in South Darfur, closed schools and power plant substations, and rendered roads impassable. The frequency and magnitude of heavy rainfall across Sudan will continue to prove a challenge for urban areas that do not have adequate infrastructure, and will ultimately compromise the economic development of the region.

Human health impacts

Rainfall is also a key component for the propagation of several vector-borne diseases relevant to Eastern Africa. Mosquitoes and other arthropods that carry malaria and arboviruses such as dengue often include an aquatic stage to support the development of their eggs and larvae. As such, ENSO^{145–148} and the IOD^{149,150} have been linked to malaria risk across the region. For example, extreme rainfall associated with the strong El Niño during 1997/1998 followed an extended drought period and led to an outbreak of malaria in a non-immune population of northeastern Kenya, the extent of which had not been seen since 1952. Records of hospital admissions reported a three-month lag after heavy rainfall in November 1997 (ref. 145). Hospital data from another community in Kenya also reported a 10-fold increase in expected daily rates of crude and under-five mortality¹⁴⁵. A similar story was reported for a district in western Uganda¹⁴⁶. For communities of the Tanzanian highlands, however, a marked reduction in malaria cases was observed in 1997/1998. This reduction was attributed to flooding, which can flush mosquito larvae from breeding sites, thereby decreasing the disease spread¹⁵¹. Two out of the three communities in Tanzania that reported an increase in malaria after the heavy rains were located next to a body of standing

water that is an ideal breeding ground for mosquitoes¹⁵¹. Water-borne diseases such as cholera and typhoid also become more of a concern during specific shifts in rainfall and variations in temperature^{143,152,153}.

Future changes

Given the multifarious impacts of rainfall changes over Eastern Africa, there is a need to consider how rainfall and its drivers might change in the future, the knowledge of which provides actionable information with which to develop effective mitigation strategies.

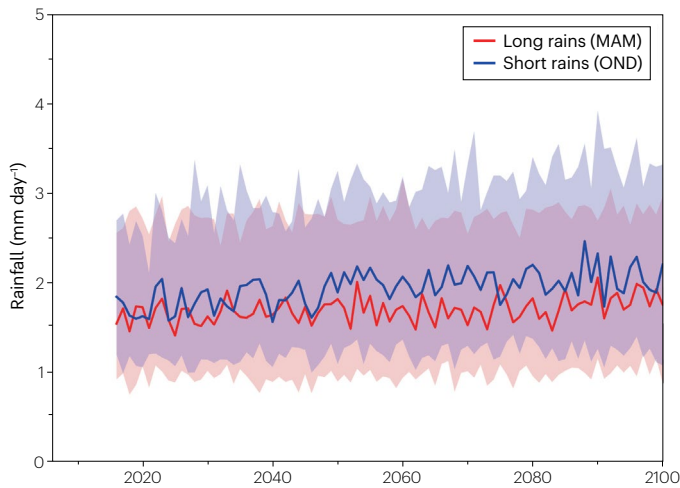
Rainfall

Global and regional climate models offer an opportunity to examine projected changes in the long and short rains^{20,50,154–160}. However, spread amongst ensemble members and models casts doubt on the reliability

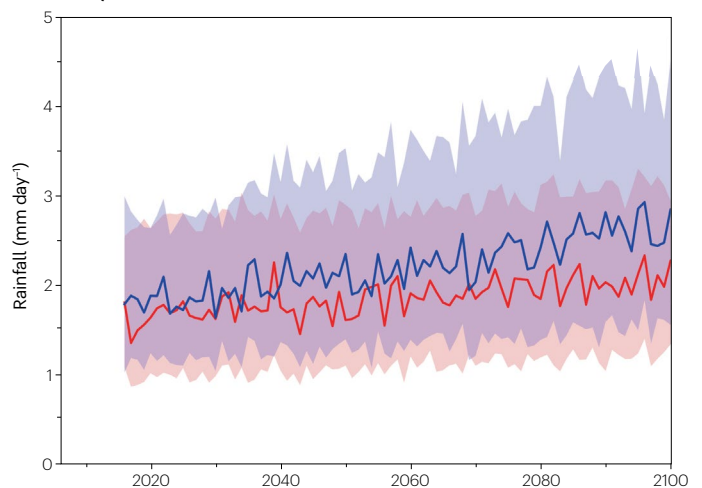
of rainfall projections⁵⁸. Moreover, given limited relationships between the abilities of individual models to describe past and future Eastern African climate and the model spread, the capability of an individual Earth system model to reproduce current-day observations provides no indication about its ability to constrain future projections¹⁶¹.

These model limitations and corresponding uncertainties are particularly evident for the long rains. Indeed, global climate models report no significant change¹⁵⁸, a decrease¹⁶² and a small increase in the long rains under anthropogenic warming, consistent with the range of responses for Coupled Model Intercomparison Project phase 5 (CMIP5)^{155,163}. CMIP6¹⁶⁴ simulations also exhibit variability, with the multimodel ensemble providing hints of a small increase (Fig. 4a,b). Under medium (Shared Socioeconomic Pathways SSP 2–4.5) and very high (SSP 5–8.5) greenhouse gas emission scenarios, for example,

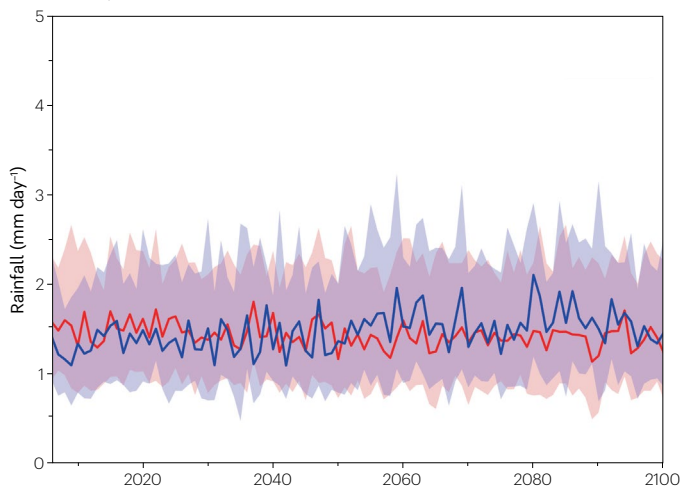
a CMIP6, SSP 2–4.5



b CMIP6, SSP 5–8.5



c CORDEX, RCP4.5



d CORDEX, RCP8.5

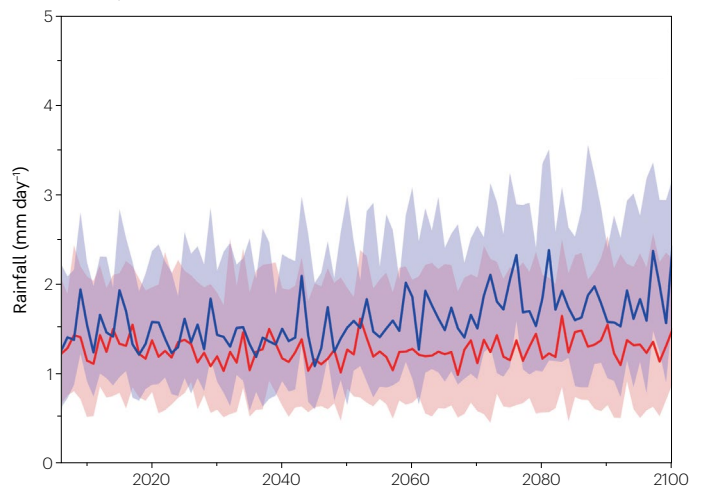


Fig. 4 | Projections of long rains and short rains. **a**, Multimodel median long rains (March–May, MAM; red) and short rains (October–December, OND; blue) projections from Coupled Model Intercomparison Project phase 6 (CMIP6) models¹⁶⁴ forced under Shared Socioeconomic Pathways SSP 2–4.5. Shading denotes the standard deviation associated with the ensemble of model runs. **b**, As in panel **a**, but for CMIP6 models forced under SSP 5–8.5. **c**, Multimodel

median long rain (MAM; red) and short rain (OND; blue) projections from CORDEX regional climate models¹⁶⁵ forced with Representative Concentration Pathway RCP4.5. **d**, As in panel **c**, but for CORDEX regional climate forced with RCP8.5. Global and regional climate model projections suggest that short rain totals will exceed those of the long rains, the timing of which depends on the future scenario.

the multimodel median projects statistically significant increases of $0.02 \text{ mm day}^{-1} \text{ decade}^{-1}$ and $0.06 \text{ mm day}^{-1} \text{ decade}^{-1}$ over 2015–2100, respectively, with changes emerging after -2080 and -2040. In contrast, CORDEX¹⁶⁵ regional models support no such increase in the long rains. Instead, they exhibit a statistically significant slight negative trend of $-0.01 \text{ mm day}^{-1} \text{ decade}^{-1}$ and a statistically insignificant positive trend of $0.01 \text{ mm day}^{-1} \text{ decade}^{-1}$ over 2006–2100 for Representative Concentration Pathways RCP4.5 and RCP8.5, respectively (Fig. 4c,d). Accordingly, there is no clear indication of the sign and magnitude of future changes in long rains, nor their potential drivers, although minimal changes have been attributed to an insensitivity of the continental thermal low to rising atmospheric GHGs¹⁵.

There is better agreement between different models and individual model ensembles for the short rains¹⁵⁵, albeit still with substantial spread, thereby providing some confidence in the projected increase with anthropogenic warming^{20,158,162}. For instance, CMIP6 models project statistically significant trends of $0.04 \text{ mm day}^{-1} \text{ decade}^{-1}$ and $0.11 \text{ mm day}^{-1} \text{ decade}^{-1}$ over 2015–2100 for SSP 2–4.5 and SSP 5–8.5, respectively (Fig. 4a,b); changes emerge in the early 2040s and 2030s for the two scenarios²⁰. CORDEX simulations exhibit a similar pattern: a small but statistically significant increase for RCP4.5 ($0.03 \text{ mm day}^{-1} \text{ decade}^{-1}$, 2006–2100; Fig. 4c), and a stronger response that emerges in the late 2040s for RCP8.5 for the same period ($0.05 \text{ mm day}^{-1} \text{ decade}^{-1}$; Fig. 4d). A convection-permitting regional model also supports these findings, additionally reporting a large increase in extreme rainfall rates during the short rains¹⁶⁶ that is not found with parameterized convection, suggesting that CMIP5, CMIP6 and CORDEX responses for extremes might be underestimated¹⁶⁶.

Enhanced moisture convergence arising from dynamic and thermodynamic¹⁵⁸ processes explains this increase in the short rains¹⁵. Dynamically, anomalous circulation patterns associated with a strengthening in the continental low over southern Africa and the subtropical high over the South Indian Ocean, and a weakening of the eastern Sahara subtropical high, drive enhanced moisture convergence. A weakening of the Walker circulation in response to warming SSTs over the western Indian Ocean also favours an upward trend in the short rains^{50,162}. Nevertheless, multiple aspects all cast doubts on rainfall projections, including: limitations in model representations of key processes and climatologies¹⁶⁷; an unrealistic dominance of the Walker circulation¹⁶⁸; and failure to reproduce the observed SST gradient across the equatorial Pacific⁵⁸. With these caveats in mind, conclusions are limited to saying that the rainfall during the short rains is increasing at a faster rate than the long rains (Fig. 4).

ENSO and IOD

Given the dominant influence of ENSO and the IOD on rainfall variations across Eastern Africa, it is instructive to understand their future projections in the hope of informing rainfall projections. As with rainfall itself, there is often a lack of consensus regarding how these modes of variability will change under anthropogenic warming. For ENSO¹⁶⁹, no significant change in intensity and frequency has been reported in some instances^{170–172}, whereas an increased occurrence of extreme El Niño and La Niña events is reported by others^{173–175}. Similarly, no significant change in the overall frequency and amplitude of the IOD is projected by coupled models^{176,177}, although the frequency of extreme positive IOD events is thought to increase^{173,178}. Assuming that present-day relationships between Eastern African rainfall and ENSO and IOD remain the same in the future, the short rains would then become wetter, with an increasing chance of torrential rains

and associated higher risk of flooding, but also the potential for groundwater recharge⁶.

Moreover, faster warming is expected in the western Indian Ocean than in surrounding bodies of water^{173,176,179}. Because of these shifts, the tropical oceans will tend towards an El Niño-like and positive IOD-like state, associated with weakening of the Walker circulation, shifts in the ITCZ¹⁸⁰ and an increase in atmospheric moist static energy. Consequently, ENSO and IOD are expected to have a stronger coupling with rainfall over the Horn of Africa but a weaker coupling with rainfall over the southern part of Eastern Africa¹⁶². The long rains, which are historically insensitive to remote SST forcing, would then become substantially more responsive to ENSO in future projections¹⁶². Model projections also suggest an enhanced La Niña-related rainfall anomaly over Eastern Africa during July–September compared with the present period¹⁶². Accordingly, if the frequency of extreme positive IOD events increases^{173,178} and the strength of the teleconnection increases over the eastern part of Eastern Africa¹⁶², wetter conditions might result over the eastern half of the region during the short rains. Yet changes in the frequency of El Niño and La Niña events, coupled with increasing sensitivity to ENSO during the long rains and summer rainfall seasons, could lead to increasing variability in these seasons in the future. Even if the frequency and intensity of ENSO and IOD do not change in a warming climate, their associated rainfall extremes can be expected to be more severe in a warming world owing to an intensified hydrological cycle¹⁸¹.

Impacts

As in the present climate, any future changes in seasonal rainfall across Eastern Africa will result in a wide range of economic and humanitarian impacts.

Changes in agricultural yields from changing rainfall patterns are crop-specific. Based on current understanding, future crop yields are more sensitive to uncertainties in temperature than rainfall⁷³, as crops generally have an optimal growing temperature range, outside which the yield falls off rapidly^{74,182}. Optimal yields also rely on adequate soil moisture that helps to regulate available water in the plant root zone¹⁸³. Changes in the timing, duration and magnitude of the long and short rains will need to be considered by farmers when they decide which crops and seed-types are grown throughout the year¹⁸⁴. Increased frequency of extreme rainfall events will result in flooding that leads to damaged crops¹⁶ and agricultural infrastructure that raises concerns about food security. Availability of water and food will also influence livestock production¹⁸⁵.

Anthropogenic warming will induce changes to large-scale biogeochemical cycles across Eastern Africa, with the possibility to feed back on atmospheric GHG concentrations¹²³. Indeed, the influence of rainfall variability on wetland methane emissions is expected to continue in the future. For instance, CMIP5-based simulations (Supplementary Information) predict that methane emissions will increase by -4 Tg yr^{-1} under RCP4.5 and -11 Tg yr^{-1} under RCP8.5 from 2000 to 2100 (Fig. 5a,b). These projected increases can be linked to increases in surface temperature, inundation (via rainfall) and net primary production (also indirectly affected by rainfall), each with similar importance (Fig. 5c). Moreover, future rainfall variability, namely the projected increase in short rains, is expected to reduce the spatial extent of fires¹⁸⁶ and enhance above-ground biomass (and associated vegetation greening¹⁸⁷ and increase in net primary production¹⁸⁸) with an accompanying transition to forest biomes over Eastern Africa^{189–191}. These changes will each have subsequent effects on ecosystem functioning, carbon cycling and broader biogeochemical storylines in the Earth system.

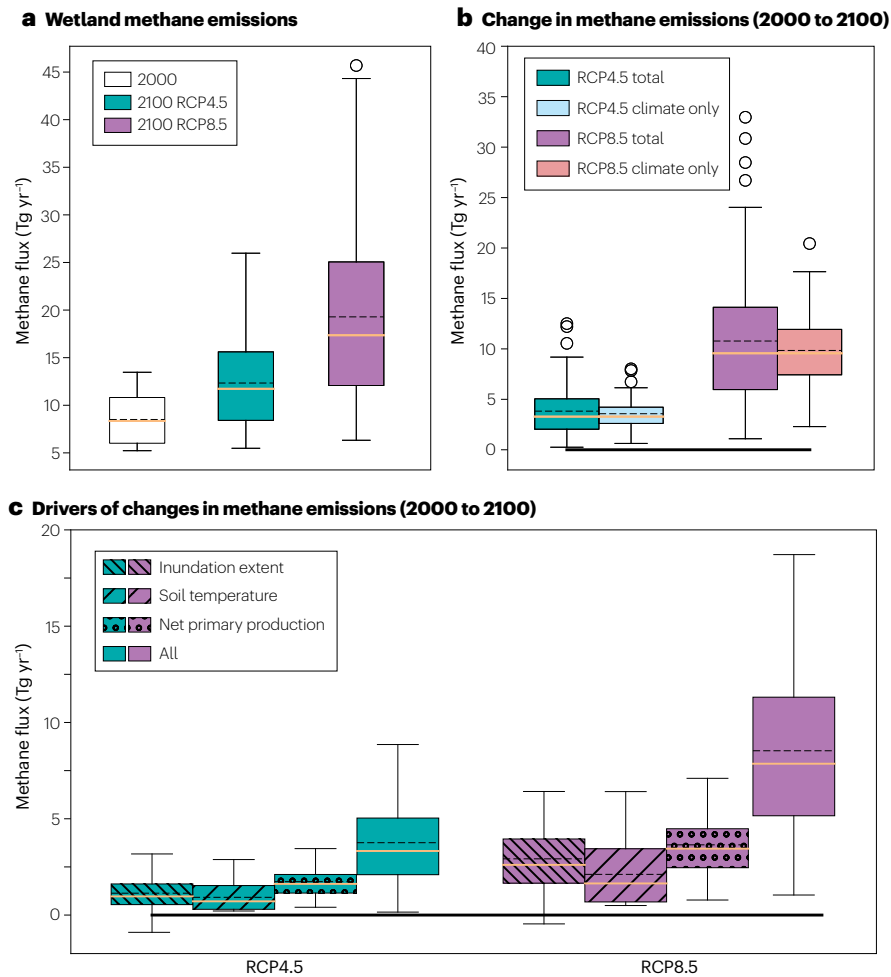


Fig. 5 | Wetland methane emissions. **a**, Methane emission estimates from the JULES model for 2000 (white) and 2100 driven by RCP4.5 (green) and RCP8.5 (magenta). **b**, Changes in methane emission estimates between 2000 and 2100 for RCP4.5 and RCP8.5. Spread due to climate uncertainty only is shown by light blue (RCP4.5) and salmon (RCP8.5) box and whiskers. **c**, Linearized estimates of changes to methane emissions from 2000 to 2100 under RCP4.5 and RCP8.5²³³ owing to inundation extent, soil temperature, net primary production and all (inundation extent plus soil temperature plus net primary production). In all cases, boxes describe the interquartile range (IQR), the whiskers the quartiles $\pm 1.5 \times$ IQR, circles outliers, and the orange and dashed black lines the mean and median values, respectively, associated with the ensemble of model runs. The solid horizontal lines in panels **b** and **c** denote the zero line. Future increases in methane emissions are driven approximately equally by warmer temperature, higher rainfall and larger net primary production.

Future changes in rainfall can also be expected to influence human health and disease. There is a threshold of relative humidity (and temperature) that limits the transmission of malaria and arboviruses via their influence on the associated vectors (for example, mosquitoes) and pathogens^{152,192,193}. Increases in relative humidity associated with more extreme wet seasons in the future can shorten the incubation and blood-feeding stages¹⁹³ of the mosquito lifecycle, but the net impact of these changes is unclear. Increased future levels of rainfall and its variability might lead to more frequent and persistent flooding that will help establish more breeding sites for insects, although some vectors breed indoors and will not be directly affected by flooding. The relationship between flooding and water-borne diseases such as cholera and typhoid differs by region^{152,192}. However, one of the biggest risks for future transmission of malaria and arboviruses in Eastern Africa is drug and insecticide resistance combined with warmer temperatures and lower relative humidity associated with climate change in the highland regions, where there is little immunity and insufficient health infrastructure^{194–197}.

Summary and future perspectives

Eastern Africa suffers extreme seasonal and year-to-year variations in rainfall, driving substantial environmental, social and economic impacts. For instance, extreme changes in hydroclimatic conditions

during 2021, exacerbated by water management challenges, have led to some of the worst flooding in South Sudan for the past 60 years, affecting food and energy security, access to potable water, and the spread of water-borne disease and arboviruses. Other parts of Eastern Africa, particularly countries in the Horn of Africa, are experiencing prolonged and extensive drought due to consecutive La Niña events from 2020 to 2022, exacerbated by GHG warming over the western Pacific. These droughts have resulted in the collapse of agricultural crops and livestock that support subsistence farming across the region.

Although uncertain, there is some consensus that short rains totals will exceed those of the long rains in a warming climate, the timing of which is dependent on the scenario but could occur as early as 2030. Regional climate models generally show a weaker rainfall response to a warming climate, yet models that resolve convection report greater intensification of extreme rainfall rates. The vast majority of climate models, which still use parameterized convection, are thus potentially underestimating future increases in rainfall and therefore the subsequent impacts across Eastern Africa.

To minimize the risks associated with extreme variations in rainfall over Eastern Africa, several priority areas of future research are required, all demanding the development of proactive policies.

Improve meteorological observing networks and forecast systems

Improved early detection and weather forecast systems that focus on Eastern Africa will engender better preparedness for extremes associated with seasonal changes in rainfall and will inform decadal planning strategies. Development and evaluation of convective-permitting regional climate models¹⁶⁶ would provide further confidence in their ability to describe extreme rainfall events that have disproportionately important impacts. Growing model skill in subseasonal rainfall forecasts^{198–204} relies on improving model physics of the atmosphere and ocean, and on more and higher-quality data, particularly from satellites with instruments that observe atmosphere and ocean properties. Improved model simulations of the long rains over Eastern Africa hinge on improving knowledge of the atmospheric state, particularly humidity, over the northwest Indian Ocean²⁰⁵, which could be tested with a dedicated measurement campaign. Ocean interior measurements currently collected by arrays of buoys across the tropics, particularly the Indian Ocean and western Pacific, could be expanded to help reduce knowledge gaps²⁰⁶. To improve forecast skill of high-impact weather events over Eastern Africa, targeted²⁰⁷ ground-based, airborne and shipborne observations could be deployed to supplement existing operational data streams. Equally important are the assimilation methods that optimize the use of these observations for improving model simulations²⁰⁸. Rescuing and sharing historical data over Africa would also improve climate predictions²⁰⁹.

Translating forecast analyses into actionable information is a key part of any system^{210,211}. The Famine Early Warning Systems Network⁸⁷ is a good example of such a system. Delivering useful information to countries requires detailed knowledge about national agricultural and economic policies, evolving national political environments, and the capability to communicate with local farming communities and governments. Establishing long-term funding that supports civilian data collecting, transcending lifecycles of individual governments, will help to provide effective information about how to mitigate the worst climate impacts.

Improve environmental observing systems

Climate and weather forecast data can also help with disease forecasting²¹², but these connections have not been fully realized. Satellite observations of surface temperature, humidity and land-use change can be used to predict shifts in disease burden²¹³ and hotspots for emerging zoonotic diseases and how they will spread^{214–216}, and together with epidemiological data could form the basis of early detection systems over Eastern Africa²¹².

Understanding quantitative changes in hydrology and the carbon cycle across Eastern Africa is currently limited to very few surface sites and broad inferences from satellite observations^{120,217}. Given the importance of water flows across the regions, and subsequent impacts on water and food security and the carbon cycle, there is a clear need for a more coordinated and sustainable measurement network to monitor variations²¹⁸. More collaboration between African and international hydrologists, ecologists and carbon-cycle scientists will help this kind of activity.

Advance Earth system models

Exploiting advances in observing systems and better understanding the carbon–water nexus must translate into commensurate improvements²¹⁰ in physically based simulations of Eastern African climate and how it relates to the broader climate system. A key recommendation is to develop a more robust understanding of the relationship between

future levels of atmospheric GHG and changes in the frequency and variability of the IOD^{69,173,176,178,219,220}, how future changes in ENSO and the IOD will influence rainfall over Eastern Africa¹⁶², and, in turn, how that influences vegetation cover and subsequently the emission of methane¹²³. This point ties together the previous recommendations. Only by bringing together communities involved in measurements and model development can meaningful progress be made with identifying and prioritizing work on reducing uncertainty.

Improve freshwater security

Eastern Africa encompasses regions that are being flooded and regions that are subject to drought, both driven by large inter- and intraseasonal changes in rainfall. In both extremes, there is an urgent need to improve national water storage infrastructure, flood protection and sanitation systems to improve the safety and security of freshwater resources that will subsequently help increase agricultural output and a growing population²²¹. Doing so is a systemic challenge that requires co-development of water-usage strategies between stakeholders and development agencies, informed by scenarios that account for changes in rainfall, land use, and the growing demands from an increase in population. Recommendations include investment in water-saving technologies and efficient management options such as the adoption of sprinkler and drip irrigation systems to replace commonly used flood irrigation, and to invest in recycling wastewater when surface or groundwater reserves are insufficient²²¹. Such an approach should also consider upstream and downstream water demands and losses, including the reduction of evaporative losses, particularly from catchment lakes and reservoirs in arid regions²²², and the potential challenges and implications of adopting different approaches²²³.

Ensure food security

Ensuring future food security is related to the security of freshwater, with the agriculture sector generally having the lowest water-use efficiency of all the water-using sectors²²⁴. How this sector will cope with changes in rainfall variability will depend on the nature of those changes. An upward trend in rainfall in some countries for different seasons, with an accompanying warming trend, might benefit some food crops that have a higher optimal growing temperature. However, if increased rainfall results from a higher frequency of extreme rainfall events that follow periods of drought, then flooding will become more of a challenge. Investment in better drainage systems is one solution, but in the longer term, an increase in flooded areas that can be managed will help provide an opportunity to increase the use of floodplain agriculture, spate irrigation²²⁵ or inundation canals. A shift in rainfall and surface water catchment areas might result in a redistribution of crops being grown across Eastern Africa. Countries that will suffer from more extensive droughts have other challenges to face. In this case, the agricultural sector should invest in strategic rainwater and surface water storage options that provide reliable flows but incur minimal additional losses, more efficient water management systems, as described above, and distributing drought-tolerant seeds²²⁶ to maximize agricultural crop yields during drought years. Widespread adoption of conservation tillage methods would reduce water and soil loss, mainly by decreasing the intensity of the tillage and retention of post-harvest plant residue²²⁷. Development of agricultural strategies to help farmers maximize food production during good years would help to mitigate impacts during drought years. Institutes affiliated with the Consultative Group on International Agricultural Research continue to play a key role in addressing those sustainable agricultural challenges.

All these recommendations require unprecedented levels of coordination and substantial financial investment to link local to national scales, and in many cases will require transboundary cooperation that will also involve extensive international diplomacy. Some activities are underway, but some countries might require international financial aid to establish larger activities that will eventually become self-sustaining. Without properly addressing the bigger challenges now, it becomes progressively more difficult for Eastern African countries to cope with future variations in rainfall without incurring substantial humanitarian and economic costs²²⁸ that will dwarf the multitrillion-dollar cost of the COVID-19 pandemic.

Published online: 21 March 2023

References

- Gamoyo, M., Reason, C. & Obura, D. Rainfall variability over the East African coast. *Theor. Appl. Climatol.* **120**, 311–322 (2015).
- World Bank Group. World Bank Open Data. <https://data.worldbank.org/>. Accessed 1 February 2023.
- OEC. Observatory of Economic Complexity. <https://oec.world/>. Accessed 1 February 2023.
- Conway, D., Dalin, C., Landman, W. A. & Osborn, T. J. Hydropower plans in eastern and southern Africa increase risk of concurrent climate-related electricity supply disruption. *Nat. Energy* **2**, 946–953 (2017).
- Ferrer, N. et al. Groundwater hydrodynamics of an Eastern Africa coastal aquifer, including La Niña 2016–17 drought. *Sci. Total Environ.* **661**, 575–597 (2019).
- Adloff, M. et al. Sustained water storage in Horn of Africa drylands dominated by seasonal rainfall extremes. *Geophys. Res. Lett.* **49**, e2022GL099299 (2022).
- Taylor, R. G. et al. Evidence of the dependence of groundwater resources on extreme rainfall in East Africa. *Nat. Clim. Change* **3**, 374–378 (2013).
- Somalia FSNAU Food Security & Nutrition Quarterly Brief — Focus on Post Gu 2017 Season Early Warning (Food Security and Nutrition Analysis Unit and Famine Early Warning System Network, 2022).
- Somalia Drought Impact and Needs Assessment: Synthesis Report (World Bank Group, 2018).
- Somalia faces Risk of Famine (IPC Phase 5) as multi-season drought and soaring food prices lead to worsening acute food insecurity and malnutrition (Food Security and Nutrition Analysis Unit, 2022); <https://fsnau.org/node/1947>.
- Horn of Africa Drought: Regional Humanitarian Overview & Call to Action (UN Office for the Coordination of Humanitarian Affairs, 2022).
- Humanitarian Needs Overview South Sudan. *Humanitarian Programme Cycle 2021* (UN Office for the Coordination of Humanitarian Affairs, 2021).
- Adhikari, U., Nejadhashemi, A. P. & Woznicki, S. A. Climate change and Eastern Africa: a review of impact on major crops. *Food Energy Secur.* **4**, 110–132 (2015).
- Megersa, B. et al. Livestock diversification: an adaptive strategy to climate and rangeland ecosystem changes in southern Ethiopia. *Hum. Ecol.* **42**, 509–520 (2014).
- Cook, K. H., Fitzpatrick, R. G. J., Liu, W. & Vizy, E. K. Seasonal asymmetry of equatorial East African rainfall projections: understanding differences between the response of the long rains and the short rains to increased greenhouse gases. *Clim. Dyn.* **55**, 1759–1777 (2020).
- Wainwright, C. M., Finney, D. L., Kilavi, M., Black, E. & Marsham, J. H. Extreme rainfall in East Africa October 2019 – January 2020 and context under future climate change. *Weather* <https://doi.org/10.1002/wea.3824> (2020).
- Black, E., Slingo, J. & Sperber, K. R. An observational study of the relationship between excessively strong short rains in coastal East Africa and Indian Ocean SST. *Mon. Weather Rev.* **131**, 74–94 (2003).
- MacLeod, D., Graham, R., O'Reilly, C., Otieno, G. & Todd, M. Causal pathways linking different flavours of ENSO with the greater Horn of Africa short rains. *Atmos. Sci. Lett.* <https://doi.org/10.1002/asl.1015> (2021).
- Indeje, M., Semazzi, F. H. M. & Ogallo, L. J. ENSO signals in East African rainfall seasons. *Int. J. Climatol.* **20**, 19–46 (2000).
- Wainwright, C. M., Marsham, J. H., Rowell, D. P., Finney, D. L. & Black, E. Future changes in seasonality in East Africa from regional simulations with explicit and parameterized convection. *J. Clim.* **34**, 1367–1385 (2021).
- Nicholson, S. E. Long-term variability of the East African 'short rains' and its links to large-scale factors. *Int. J. Climatol.* **35**, 4259 (2015).
- Jiang, Y., Zhou, L., Roundy, P. E., Hua, W. & Raghavendra, A. Increasing influence of Indian Ocean Dipole on precipitation over Central Equatorial Africa. *Geophys. Res. Lett.* **48**, e2020GL092370 (2021).
- Funk, C. et al. Examining the role of unusually warm Indo-Pacific sea-surface temperatures in recent African droughts. *Q. J. R. Meteorol. Soc.* **144**, 3266 (2018).
- Shaaban, A. A. & Roundy, P. E. OLR perspective on the Indian Ocean Dipole with application to East African precipitation. *Q. J. R. Meteorol. Soc.* **143**, 3045 (2017).
- Zaitchik, B. F. Madden-Julian Oscillation impacts on tropical African precipitation. *Atmos. Res.* **184**, 88–102 (2017).
- Pohl, B. & Camberlin, P. Influence of the Madden-Julian Oscillation on East African rainfall. I: Intraseasonal variability and regional dependency. *Q. J. R. Meteorol. Soc.* **132**, 104 (2006).
- Finney, D. L. et al. The effect of westerlies on East African rainfall and the associated role of tropical cyclones and the Madden-Julian Oscillation. *Q. J. R. Meteorol. Soc.* **146**, 3698 (2020).
- Pohl, B. & Camberlin, P. Influence of the Madden-Julian Oscillation on East African rainfall. II: March–May season extremes and interannual variability. *Q. J. R. Meteorol. Soc.* **132**, 223 (2006).
- Berhane, F. & Zaitchik, B. Modulation of daily precipitation over East Africa by the Madden-Julian oscillation. *J. Clim.* **27**, 1 (2014).
- Vellinga, M. & Milton, S. F. Drivers of interannual variability of the East African 'Long Rains'. *Q. J. R. Meteorol. Soc.* **144**, 861–876 (2018).
- Martin, Z. et al. The influence of the quasi-biennial oscillation on the Madden-Julian oscillation. *Nat. Rev. Earth Environ.* **2**, 477–489 (2021).
- Gelaro, R. et al. The Modern-Era Retrospective Analysis for Research and Applications, version 2 (MERRA-2). *J. Clim.* **30**, 5419–5454 (2017).
- Huesmann, A. S. & Hitchman, M. H. The stratospheric quasi-biennial oscillation in the NCEP reanalyses: climatological structures. *J. Geophys. Res. Atmos.* **106**, 11859–11874 (2001).
- Indeje, M. & Semazzi, F. H. M. Relationships between QBO in the lower equatorial stratospheric zonal winds and East African seasonal rainfall. *Meteorol. Atmos. Phys.* **73**, 580 (2000).
- Liu, W., Cook, K. H. & Vizy, E. K. Influence of Indian Ocean SST regionality on the East African short rains. *Clim. Dyn.* **54**, 4991–5011 (2020).
- Dyer, E. & Washington, R. Kenyan long rains: a subseasonal approach to process-based diagnostics. *J. Clim.* **34**, 1–48 (2021).
- Kilavi, M. et al. Extreme rainfall and flooding over Central Kenya including Nairobi City during the long-rains season 2018: causes, predictability, and potential for early warning and actions. *Atmosphere* **9**, 472 (2018).
- Kebacho, L. L. The role of tropical cyclones Ildai and Kenneth in modulating rainfall performance of 2019 long rains over East Africa. *Pure Appl. Geophys.* **179**, 1387–1401 (2022). (2022).
- Kebacho, L. L. Interannual variations of the monthly rainfall anomalies over Tanzania from March to May and their associated atmospheric circulations anomalies. *Nat. Hazards* **112**, 163–186 (2022).
- Tarnavsky, E. et al. Extension of the TAMSAT satellite-based rainfall monitoring over Africa and from 1983 to present. *J. Appl. Meteorol. Climatol.* **53**, 2805–2822 (2014).
- Maidment, R. I. et al. A new, long-term daily satellite-based rainfall dataset for operational monitoring in Africa. *Sci. Data* **4**, 170063 (2017).
- Dai, A. Hydroclimatic trends during 1950–2018 over global land. *Clim. Dyn.* **56**, 4027–4049 (2021).
- Maidment, R. I., Allan, R. P. & Black, E. Recent observed and simulated changes in precipitation over Africa. *Geophys. Res. Lett.* **42**, 8155–8164 (2015).
- Cattani, E., Merino, A., Guijarro, J. A. & Levizzani, V. East Africa rainfall trends and variability 1983–2015 using three long-term satellite products. *Remote Sens.* **10**, 931 (2018).
- Maidment, R. I. et al. The 30 year TAMSAT African rainfall climatology and time series (TARCAT) data set. *J. Geophys. Res.* **119**, 10619–10644 (2014).
- Liebmann, B. et al. Climatology and interannual variability of boreal spring wet season precipitation in the eastern Horn of Africa and implications for its recent decline. *J. Clim.* **30**, 3867–3886 (2017).
- Wainwright, C. M. et al. 'Eastern African Paradox' rainfall decline due to shorter not less intense long rains. *npj Clim. Atmos. Sci.* **2**, 34 (2019).
- Walker, D. P., Marsham, J. H., Birch, C. E., Scaife, A. A. & Finney, D. L. Common mechanism for interannual and decadal variability in the East African long rains. *Geophys. Res. Lett.* **47**, e2020GL089182 (2020).
- Nicholson, S. E. Climate and climatic variability of rainfall over Eastern Africa. *Rev. Geophys.* **55**, 590–635 (2017).
- Tierney, J. E., Ummenhofer, C. C. & deMenocal, P. B. Past and future rainfall in the Horn of Africa. *Sci. Adv.* **1**, e1500682 (2015).
- Saji, N. H., Goswami, B. N., Vinayachandran, P. N. & Yamagata, T. A dipole mode in the tropical Indian Ocean. *Nature* **401**, 360–363 (1999).
- Webster, P. J., Moore, A. M., Loschnigg, J. P. & Leben, R. R. Coupled ocean-atmosphere dynamics in the Indian Ocean during 1997–98. *Nature* **401**, 356–360 (1999).
- Funk, C. et al. Examining the potential contributions of extreme 'Western V' sea surface temperatures to the 2017 March–June East African drought. *Bull. Am. Meteorol. Soc.* **100**, S55–S60 (2019).
- Thielke, A. & Mölg, T. Observed and simulated Indian Ocean Dipole activity since the mid-19th century and its relation to East African short rains. *Int. J. Climatol.* **39**, 4467–4478 (2019).
- Trenberth, K. E., Fasullo, J. T., Branstator, G. & Phillips, A. S. Seasonal aspects of the recent pause in surface warming. *Nat. Clim. Change* **4**, 911–916 (2014).
- L'Heureux, M. L., Lee, S. & Lyon, B. Recent multidecadal strengthening of the Walker circulation across the tropical Pacific. *Nat. Clim. Change* **3**, 571–576 (2013).
- England, M. H. et al. Recent intensification of wind-driven circulation in the Pacific and the ongoing warming hiatus. *Nat. Clim. Change* **4**, 222–227 (2014).
- Seager, R. et al. Strengthening tropical Pacific zonal sea surface temperature gradient consistent with rising greenhouse gases. *Nat. Clim. Change* **9**, 517–522 (2019).

59. Black, E. The relationship between Indian Ocean sea-surface temperature and East African rainfall. *Phil. Trans. R. Soc. A* **363**, 43–47 (2005).
60. Liebmann, B. et al. Understanding recent eastern Horn of Africa rainfall variability and change. *J. Clim* **27**, 8630–8645 (2014).
61. Lyon, B. Seasonal drought in the Greater Horn of Africa and its recent increase during the March–May long rains. *J. Clim* **27**, 7953–7975 (2014).
62. Allan, R. P. et al. Advances in understanding large-scale responses of the water cycle to climate change. *Ann. N. Y. Acad. Sci.* **1472**, 49–75 (2020).
63. Bronnimann, S. et al. Southward shift of the northern tropical belt from 1945 to 1980. *Nat. Geosci.* **8**, 969–974 (2015).
64. Undorf, S. et al. Detectable impact of local and remote anthropogenic aerosols on the 20th century changes of West African and South Asian monsoon precipitation. *J. Geophys. Res. Atmos.* **123**, 4871–4889 (2018).
65. Dong, B. & Sutton, R. Dominant role of greenhouse-gas forcing in the recovery of Sahel rainfall. *Nat. Clim. Change* **5**, 757–760 (2015).
66. Blau, M. T. & Ha, K. J. The Indian Ocean Dipole and its impact on East African short rains in two CMIP5 historical scenarios with and without anthropogenic influence. *J. Geophys. Res. Atmos.* **125**, e2020JD033121 (2020).
67. Kew, S. F. et al. Impact of precipitation and increasing temperatures on drought trends in eastern Africa. *Earth Syst. Dyn.* **12**, 17–35 (2021).
68. Held, I. M. & Soden, B. J. Robust responses of the hydrological cycle to global warming. *J. Clim* **19**, 5686–5699 (2006).
69. Vecchi, G. A. & Soden, B. J. Global warming and the weakening of the tropical circulation. *J. Clim* **20**, 73–76 (2007).
70. Byrne, M. P. & Schneider, T. Narrowing of the ITCZ in a warming climate: physical mechanisms. *Geophys. Res. Lett.* **43**, 11350–11357 (2016).
71. Byrne, M. P., Pendergrass, A. G., Rapp, A. D. & Wodzicki, K. R. Response of the intertropical convergence zone to climate change: location, width, and strength. *Curr. Clim. Change Rep.* **4**, 355–370 (2018).
72. Chemura, A., Mudereri, B. T., Yalew, A. W. & Gornott, C. Climate change and specialty coffee potential in Ethiopia. *Sci. Rep.* **11**, 8097 (2021).
73. Lobell, D. B. & Burke, M. B. Why are agricultural impacts of climate change so uncertain? The importance of temperature relative to precipitation. *Environ. Res. Lett.* **3**, 034007 (2008).
74. Tigchelaar, M., Battisti, D. S., Naylor, R. L. & Ray, D. K. Future warming increases probability of globally synchronized maize production shocks. *Proc. Natl Acad. Sci. USA* **115**, 6644–6649 (2018).
75. Shapiro, L. L. M., Whitehead, S. A. & Thomas, M. B. Quantifying the effects of temperature on mosquito and parasite traits that determine the transmission potential of human malaria. *PLoS Biol.* **15**, 2003489 (2017).
76. Ayana, E. K., Ceccato, P., Fisher, J. R. B. & DeFries, R. Examining the relationship between environmental factors and conflict in pastoralist areas of East Africa. *Sci. Total Environ.* **557–558**, 601–611 (2016).
77. Nakawuka, P., Langan, S., Schmitter, P. & Barron, J. A review of trends, constraints and opportunities of smallholder irrigation in East Africa. *Glob. Food Sec.* **17**, 196–212 (2018).
78. Alter, R. E., Im, E. S. & Eltahir, E. A. B. Rainfall consistently enhanced around the Gezira Scheme in East Africa due to irrigation. *Nat. Geosci.* **8**, 763–767 (2015).
79. Vicente-Serrano, S. M. et al. Challenges for drought mitigation in Africa: the potential use of geospatial data and drought information systems. *Appl. Geogr.* **34**, 471–486 (2012).
80. Mera, G. A. Drought and its impacts in Ethiopia. *Weather. Clim. Extrem.* **22**, 24–35 (2018).
81. Funk, C. Ethiopia, Somalia and Kenya face devastating drought. *Nature* **566**, 645 (2020).
82. Philip, S. et al. *The Drought in Ethiopia* (Climate and Development Knowledge Network and World Weather Attribution Initiative, 2015); <https://cdkn.org/sites/default/files/files/Ethiopia-drought-science-summary.pdf>.
83. Toreti, A. et al. *Drought in East Africa August 2022*. GDO Analytical Report (GDO, 2022).
84. Bachewe, F. N., Yimer, F., Minten, B. & Dorosh, P. A. *Agricultural prices during drought in Ethiopia*. ESSP Working Paper Vol. 97 (2016).
85. Obasi, G. O. P. in *Climate Change and Africa* (ed. Low, P. S.) 218–230 (Cambridge Univ. Press, 2005).
86. Desta, Z. H. & Oba, G. Feed scarcity and livestock mortality in enset farming systems in the Bale highlands of southern Ethiopia. *Outlook Agric.* **33**, 277–280 (2004).
87. Funk, C. et al. Recognizing the Famine Early Warning Systems Network over 30 years of drought early warning science advances and partnerships promoting global food security. *Bull. Am. Meteorol. Soc.* **100**, 1011–1027 (2019).
88. Novella, N. S. & Thiaw, W. M. African rainfall climatology version 2 for famine early warning systems. *J. Appl. Meteorol. Climatol.* **52**, 588–606 (2013).
89. Backer, D. & Billing, T. Validating Famine Early Warning Systems Network projections of food security in Africa, 2009–2020. *Glob. Food Sec.* **29**, 100510 (2021).
90. Simtowe, F. et al. Heterogeneous seed access and information exposure: implications for the adoption of drought-tolerant maize varieties in Uganda. *Agric. Food Econ.* **7**, 15 (2019).
91. Korecha, D. & Barnston, A. G. Predictability of June–September rainfall in Ethiopia. *Mon. Weather Rev.* **135**, 628–650 (2007).
92. Yang, M. et al. The role of climate in the trend and variability of Ethiopia's cereal crop yields. *Sci. Total Environ.* **723**, 137893 (2020).
93. Wilkes, M. A. et al. Physical and biological controls on fine sediment transport and storage in rivers. *Wiley Interdiscip. Rev. Water* **6**, e1331 (2019).
94. Gebrehiwot, K. A. A review on waterlogging, salinization and drainage in Ethiopian irrigated agriculture. *Sustain. Water Resour. Manag.* **4**, 55–62 (2018).
95. Fenta, A. A. et al. Cropland expansion outweighs the monetary effect of declining natural vegetation on ecosystem services in sub-Saharan Africa. *Ecosyst. Serv.* **45**, 101154 (2020).
96. Showler, A. T. Locust 1 (Orthoptera: Acrididae) outbreak in Africa and Asia, 1992–1994: an overview. *Am. Entomol.* **41**, 179–185 (1995).
97. Foster, Z. J. The 1915 locust attack in Syria and Palestine and its role in the famine during the First World War. *Middle East. Stud.* **51**, 370–394 (2015).
98. Showler, A. T. & Potter, C. S. Synopsis of the 1986–1989 desert locust (Orthoptera: Acrididae) plague and the concept of strategic control. *Am. Entomol.* **37**, 106–110 (1991).
99. Bennett, L. V. The development and termination of the 1968 plague of the desert locust, *Schistocerca gregaria* (Forskål) (Orthoptera, Acrididae). *Bull. Entomol. Res.* **66**, 511–552 (1976).
100. *Impact of Desert Locust Infestation on Household Livelihoods and Food Security in Ethiopia: Joint Assessment Findings* (FAO, 2020).
101. Kray, H. & Shetty, S. The locust plague: fighting a crisis within a crisis (World Bank blog, 2020).
102. IPC Alert on Locusts. *IPC* (12 February 2020); <https://www.ipcinfo.org/ipcinfo-website/ipc-alerts/issue-18/en/>.
103. Madani, N. et al. Below-surface water mediates the response of African forests to reduced rainfall. *Environ. Res. Lett.* **15**, 034063 (2020).
104. Guan, K. et al. Photosynthetic seasonality of global tropical forests constrained by hydroclimate. *Nat. Geosci.* **8**, 284–289 (2015).
105. Madani, N., Kimball, J. S., Jones, L. A., Parazoo, N. C. & Guan, K. Global analysis of bioclimatic controls on ecosystem productivity using satellite observations of solar-induced chlorophyll fluorescence. *Remote. Sens.* **9**, 530 (2017).
106. Jones, L. A. et al. The SMAP Level 4 carbon product for monitoring ecosystem land-atmosphere CO₂ exchange. *IEEE Trans. Geosci. Remote. Sens.* **55**, 6517–6532 (2017).
107. Bauer, S. E., Im, U., Mezuman, K. & Gao, C. Y. Desert dust, industrialization, and agricultural fires: health impacts of outdoor air pollution in Africa. *J. Geophys. Res. Atmos.* **124**, 4104–4120 (2019).
108. Jaegle, L., Steinberger, L., Martin, R. V. & Chance, K. Global partitioning of NO_x sources using satellite observations: relative roles of fossil fuel combustion, biomass burning and soil emissions. *Faraday Discuss.* **130**, 407–423 (2005).
109. van der Werf, G. R. et al. Global fire emissions estimates during 1997–2016. *Earth Syst. Sci. Data* **9**, 697–720 (2017).
110. Bistinas, I., Harrison, S. P., Prentice, I. C. & Pereira, J. M. C. Causal relationships versus emergent patterns in the global controls of fire frequency. *Biogeosciences* **11**, 81188 (2014).
111. Finney, D. L. et al. African lightning and its relation to rainfall and climate change in a convection-permitting model. *Geophys. Res. Lett.* **47**, e2020GL088163 (2020).
112. Andela, N. et al. A human-driven decline in global burned area. *Science* **356**, 1356–1362 (2017).
113. Andela, N. & Van Der Werf, G. R. Recent trends in African fires driven by cropland expansion and El Niño to la Niña transition. *Nat. Clim. Change* **4**, 791–795 (2014).
114. Chen, Y. et al. A pan-tropical cascade of fire driven by El Niño/Southern Oscillation. *Nat. Clim. Change* **7**, 906–911 (2017).
115. Kim, I. W. et al. Tropical Indo-Pacific SST influences on vegetation variability in eastern Africa. *Sci. Rep.* **11**, 10462 (2021).
116. Ringeval, B. et al. An attempt to quantify the impact of changes in wetland extent on methane emissions on the seasonal and interannual time scales. *Global Biogeochem. Cycles* <https://doi.org/10.1029/2008GB003354> (2010).
117. Bloom, A. A., Palmer, P. I., Fraser, A., David, S. R. & Frankenberg, C. Large-scale controls of methanogenesis inferred from methane and gravity spaceborne data. *Science* **327**, 322–325 (2010).
118. Van Damme, M. et al. Industrial and agricultural ammonia point sources exposed. *Nature* **564**, 99–103 (2018).
119. Dammers, E. et al. NH₃ emissions from large point sources derived from CrIS and IASI satellite observations. *Atmos. Chem. Phys.* **19**, 12261–12293 (2019).
120. Lunt, M. F. et al. An increase in methane emissions from tropical Africa between 2010 and 2016 inferred from satellite data. *Atmos. Chem. Phys.* **19**, 14721–14740 (2019).
121. Lunt, M. F. et al. Rain-fed pulses of methane from East Africa during 2018–2019 contributed to atmospheric growth rate. *Environ. Res. Lett.* **16**, 24021 (2021).
122. Pandey, S. et al. Using satellite data to identify the methane emission controls of South Sudan's wetlands. *Biogeosciences* **18**, 557–572 (2021).
123. Feng, L., Palmer, P. I., Zhu, S., Parker, R. J. & Liu, Y. Tropical methane emissions explain large fraction of recent changes in global atmospheric methane growth rate. *Nat. Commun.* **13**, 1378 (2022).
124. Qu, Z. et al. Attribution of the 2020 surge in atmospheric methane by inverse analysis of GOSAT observations. *Environ. Res. Lett.* **17**, 094003 (2022).
125. Feng, L., Palmer, P. I., Parker, R. J., Lunt, M. F. & Boesch, H. Methane emissions responsible for record-breaking atmospheric methane growth rates in 2020 and 2021. *Atmos. Chem. Phys. Discuss.* **2022**, 1–23 (2022).
126. Koutsogiannis, D., Yao, H. & Georgakakos, A. Medium-range flow prediction for the Nile: a comparison of stochastic and deterministic methods/Prévision du débit du Nil à moyen terme: une comparaison de méthodes stochastiques et déterministes. *Hydro. Sci. J.* **53**, 142–164 (2008).
127. Kim, M. & Or, D. Microscale pH variations during drying of soils and desert biocrusts affect HONO and NH₃ emissions. *Nat. Commun.* **10**, 3944 (2019).

128. Roelle, P. A. & Aneja, V. P. Characterization of ammonia emissions from soils in the upper coastal plain, North Carolina. *Atmos. Environ.* **36**, 35–42 (2002).
129. Clarisse, L. et al. Atmospheric ammonia (NH₃) emanations from Lake Natron's saline mudflats. *Sci. Rep.* **9**, 4441 (2019).
130. Hickman, J. E. et al. Changes in biomass burning, wetland extent, or agriculture drive atmospheric NH₃ trends in select African regions. *Atmos. Chem. Phys.* **21**, 16277–16291 (2021).
131. Di Vittorio, C. A. & Georgakakos, A. P. Land cover classification and wetland inundation mapping using MODIS. *Remote. Sens. Environ.* **204**, 1–17 (2018).
132. Sridharan, V. et al. Resilience of the Eastern African electricity sector to climate driven changes in hydropower generation. *Nat. Commun.* **10**, 302 (2019).
133. Jeuland, M. Economic implications of climate change for infrastructure planning in transboundary water systems: an example from the Blue Nile. *Water Resour. Res.* **46**, W11556 (2010).
134. Jeuland, M. & Whittington, D. Water resources planning under climate change: assessing the robustness of real options for the Blue Nile. *Water Resour. Res.* **50**, 2086–2107 (2014).
135. Siderius, C. et al. Hydrological response and complex impact pathways of the 2015/2016 El Niño in Eastern and Southern Africa. *Earth's Futur.* **6**, 2–22 (2018).
136. Samboko, P. et al. *The Impact of Power Rationing on Zambia's Agricultural Sector*. No. 1093-2016-87940 (Indaba Agricultural Policy Research Institute, 2016).
137. Dinar, A., Blankespoor, B., Dinar, S. & Kurukulasuriya, P. Does precipitation and runoff variability affect treaty cooperation between states sharing international bilateral rivers? *Ecol. Econ.* **69**, 2568–2581 (2010).
138. Wheeler, K. G., Jeuland, M., Hall, J. W., Zagana, E. & Whittington, D. Understanding and managing new risks on the Nile with the Grand Ethiopian Renaissance Dam. *Nat. Commun.* **11**, 5222 (2020).
139. Wheeler, K. G. et al. Cooperative filling approaches for the Grand Ethiopian Renaissance Dam. *Water Int.* **41**, 611–634 (2016).
140. Peña-Ramos, J. A., José López-Bedmar, R., Sastre, F. J. & Martínez-Martínez, A. Water conflicts in Sub-Saharan Africa. *Front. Environ. Sci.* <https://doi.org/10.3389/fenvs.2022.863903> (2022).
141. Douglas, I. et al. Unjust waters: climate change, flooding and the urban poor in Africa. *Environ. Urban.* **20**, 187–205 (2008).
142. Birhanu, D., Kim, H., Jang, C. & Park, S. Flood risk and vulnerability of Addis Ababa City due to climate change and urbanization. *Procedia Eng.* **154**, 696–702 (2016).
143. Mahmood, M. I., Elagib, N. A., Horn, F. & Saad, S. A. G. Lessons learned from Khartoum flash flood impacts: an integrated assessment. *Sci. Total Environ.* **601–602**, 1031–1045 (2017).
144. African Research Bulletin. Flooding: Sudan. *Afr. Res. Bull. Econ. Financ. Tech. Ser.* **57**, 23103A–23106C (2020).
145. Brown, V., Issak, M. A., Rossi, M., Barboza, P. & Paugam, A. Epidemic of malaria in north-eastern Kenya. *Lancet* **352**, 1356–1357 (1998).
146. Kilian, A. H. D., Langi, P., Talisuna, A. & Kabagambe, G. Rainfall pattern, El Niño and malaria in Uganda. *Trans. R. Soc. Trop. Med. Hyg.* **93**, 22–23 (1999).
147. Boyce, R. et al. Severe flooding and malaria transmission in the Western Ugandan Highlands: implications for disease control in an era of global climate change. *J. Infect. Dis.* **214**, 1403–1410 (2016).
148. Nosrat, C. et al. Impact of recent climate extremes on mosquito-borne disease transmission in Kenya. *PLoS Negl. Trop. Dis.* **15**, 0009182 (2021).
149. Hashizume, M., Terao, T. & Minakawa, N. The Indian Ocean Dipole and malaria risk in the highlands of western Kenya. *Proc. Natl Acad. Sci. USA* <https://doi.org/10.1073/pnas.0806544106> (2009).
150. Hashizume, M., Chaves, L. F. & Minakawa, N. Indian Ocean Dipole drives malaria resurgence in East African highlands. *Sci. Rep.* **2**, 269 (2012).
151. Lindsay, S. W., Bøedker, R., Malima, R., Msangeni, H. A. & Kisinza, W. Effect of 1997–98 El Niño on highland malaria in Tanzania. *Lancet* **355**, 989–990 (2000).
152. Moore, S. M. et al. El Niño and the shifting geography of cholera in Africa. *Proc. Natl Acad. Sci. USA* <https://doi.org/10.1073/pnas.1617218114> (2017).
153. Rieckmann, A., Tamason, C. C., Gurlley, E. S., Rod, N. H. & Jensen, P. K. M. Exploring droughts and floods and their association with cholera outbreaks in Sub-Saharan Africa: a register-based ecological study from 1990 to 2010. *Am. J. Trop. Med. Hyg.* **98**, 1269–1274 (2018).
154. Yang, W., Seager, R., Cane, M. A. & Lyon, B. The East African long rains in observations and models. *J. Clim.* **27**, 7185–7202 (2014).
155. Rowell, D. P., Booth, B. B. B., Nicholson, S. E. & Good, P. Reconciling past and future rainfall trends over East Africa. *J. Clim.* **28**, 9768–9788 (2015).
156. Dunning, C. M., Black, E. & Allan, R. P. Later wet seasons with more intense rainfall over Africa under future climate change. *J. Clim.* **31**, 9719–9738 (2018).
157. Makula, E. K. & Zhou, B. Coupled Model Intercomparison Project phase 6 evaluation and projection of East African precipitation. *Int. J. Climatol.* **42**, 2398–2412 (2021).
158. Cook, B. I. et al. Twenty-first century drought projections in the CMIP6 forcing scenarios. *Earth's Future* <https://doi.org/10.1029/2019EF001461> (2020).
159. Ongoma, V., Chena, H. & Gao, C. Projected changes in mean rainfall and temperature over east Africa based on CMIP5 models. *Int. J. Climatol.* **38**, 1375–1392 (2018).
160. Akinsanola, A. A., Ongoma, V. & Koopman, G. J. Evaluation of CMIP6 models in simulating the statistics of extreme precipitation over Eastern Africa. *Atmos. Res.* **254**, 105509 (2021).
161. Rowell, D. P., Senior, C. A., Vellinga, M. & Graham, R. J. Can climate projection uncertainty be constrained over Africa using metrics of contemporary performance? *Clim. Change* **134**, 621–633 (2016).
162. Endris, H. S. et al. Future changes in rainfall associated with ENSO, IOD and changes in the mean state over Eastern Africa. *Clim. Dyn.* **52**, 2029–2053 (2019).
163. Ayugi, B. et al. Comparison of CMIP6 and CMIP5 models in simulating mean and extreme precipitation over East Africa. *Int. J. Climatol.* **41**, 6474–6496 (2021).
164. Eyring, V. et al. Overview of the Coupled Model Intercomparison Project phase 6 (CMIP6) experimental design and organization. *Geosci. Model. Dev.* **9**, 1937–1958 (2016).
165. Iturbide, M. et al. Repository supporting the implementation of FAIR principles in the IPCC-WG1 Atlas. <https://doi.org/10.5281/zenodo.3691645> (2021).
166. Finney, D. L. et al. Effects of explicit convection on future projections of mesoscale circulations, rainfall, and rainfall extremes over Eastern Africa. *J. Clim.* **33**, 2701–2718 (2020).
167. Lyon, B. Biases in sea surface temperature and the annual cycle of greater Horn of Africa rainfall in CMIP6. *Int. J. Climatol.* **42**, 4179–4186 (2021).
168. King, J. A., Washington, R. & Engelstaedter, S. Representation of the Indian Ocean Walker circulation in climate models and links to Kenyan rainfall. *Int. J. Climatol.* **41**, 6714 (2021).
169. Cai, W. et al. Changing El Niño–Southern Oscillation in a warming climate. *Nat. Rev. Earth Environ.* **2**, 628–644 (2021).
170. Zelle, H., van Oldenborgh, G. J., Burgers, G. & Dijkstra, H. El Niño and greenhouse warming: results from ensemble simulations with the NCAR CCSM. *J. Clim.* **18**, 4669–4683 (2005).
171. Merryfield, W. J. Changes to ENSO under CO₂ doubling in a multimodel ensemble. *J. Clim.* **19**, 4009–4027 (2006).
172. Collins, M. et al. The impact of global warming on the tropical Pacific Ocean and El Niño. *Nat. Geosci.* **3**, 391–397 (2010).
173. Cai, W. et al. Increasing frequency of extreme El Niño events due to greenhouse warming. *Nat. Clim. Change* **4**, 111–116 (2014).
174. Cai, W. et al. ENSO and greenhouse warming. *Nat. Clim. Change* **5**, 849–859 (2015).
175. Singh, J. et al. Enhanced risk of concurrent regional droughts with increased ENSO variability and warming. *Nat. Clim. Change* **12**, 163–170 (2022).
176. Zheng, X. T. et al. Indian Ocean Dipole response to global warming in the CMIP5 multimodel ensemble. *J. Clim.* **26**, 6067–6080 (2013).
177. Cai, W. & Cowan, T. Why is the amplitude of the Indian Ocean Dipole overly large in CMIP3 and CMIP5 climate models? *Geophys. Res. Lett.* **40**, 1200–1205 (2013).
178. Cai, W. et al. Opposite response of strong and moderate positive Indian Ocean Dipole to global warming. *Nat. Clim. Change* **11**, 27–32 (2021).
179. Chu, J. E. et al. Future change of the Indian Ocean basin-wide and dipole modes in the CMIP5. *Clim. Dyn.* **43**, 535–551 (2014).
180. Mamlakis, A. et al. Zonally contrasting shifts of the tropical rain belt in response to climate change. *Nat. Clim. Change* **11**, 143–151 (2021).
181. IPCC *Climate Change 2021: The Physical Science Basis* (eds. Masson-Delmotte, V. et al.) 1055–1210 (IPCC, Cambridge Univ. Press, 2021).
182. Schlenker, W. & Roberts, M. J. Nonlinear temperature effects indicate severe damages to U.S. crop yields under climate change. *Proc. Natl Acad. Sci. USA* **106**, 15594–15598 (2009).
183. Wang, X., Xie, H., Guan, H. & Zhou, X. Different responses of MODIS-derived NDVI to root-zone soil moisture in semi-arid and humid regions. *J. Hydrol.* **340**, 476–490 (2007).
184. Guido, Z. et al. Farmer forecasts: impacts of seasonal rainfall expectations on agricultural decision-making in sub-Saharan Africa. *Clim. Risk Manag.* **30**, 100247 (2020).
185. Thornton, P. K., van de Steeg, J., Notenbaert, A. & Herrero, M. The impacts of climate change on livestock and livestock systems in developing countries: a review of what we know and what we need to know. *Agric. Syst.* **101**, 822–825 (2009).
186. Senande-Rivera, M., Insua-Costa, D. & Miguez-Macho, G. Spatial and temporal expansion of global wildland fire activity in response to climate change. *Nat. Commun.* **13**, 1208 (2022).
187. Piao, S. et al. Characteristics, drivers and feedbacks of global greening. *Nat. Rev. Earth Environ.* **1**, 14–27 (2020).
188. Zarei, A., Chemura, A., Gleixner, S. & Hoff, H. Evaluating the grassland NPP dynamics in response to climate change in Tanzania. *Ecol. Indic.* **125**, 107600 (2021).
189. Martens, C. et al. Large uncertainties in future biome changes in Africa call for flexible climate adaptation strategies. *Glob. Change Biol.* **27**, 340–358 (2021).
190. Doherty, R. M., Sitch, S., Smith, B., Lewis, S. L. & Thornton, P. K. Implications of future climate and atmospheric CO₂ content for regional biogeochemistry, biogeography and ecosystem services across East Africa. *Glob. Change Biol.* **16**, 617–640 (2010).
191. Scheiter, S. & Higgins, S. I. Impacts of climate change on the vegetation of Africa: an adaptive dynamic vegetation modelling approach. *Glob. Change Biol.* **15**, 2224–2246 (2009).
192. Kim, J. H. et al. A systematic review of typhoid fever occurrence in Africa. *Clin. Infect. Dis.* **69**, S492–S498 (2019).
193. Lahondre, C. & Lazzari, C. R. Mosquitoes cool down during blood feeding to avoid overheating. *Curr. Biol.* **22**, 40–45 (2012).
194. Endo, N. & Eltahir, E. A. B. Increased risk of malaria transmission with warming temperature in the Ethiopian highlands. *Environ. Res. Lett.* **15**, 54006 (2020).
195. Caminade, C., McIntyre, K. M. & Jones, A. E. Impact of recent and future climate change on vector-borne diseases. *Ann. N. Y. Acad. Sci.* **1436**, 157–173 (2019).
196. Colón-González, F. J. et al. Projecting the risk of mosquito-borne diseases in a warmer and more populated world: a multi-model, multi-scenario intercomparison modelling study. *Lancet Planet. Heal.* **5**, e404–e414 (2021).
197. Ryan, S. J., Lippi, C. A. & Zermoglio, F. Shifting transmission risk for malaria in Africa with climate change: a framework for planning and intervention. *Malar. J.* **19**, 170 (2020).

198. Kolstad, E. W., MacLeod, D. & Demissie, T. D. Drivers of subseasonal forecast errors of the East African short rains. *Geophys. Res. Lett.* **48**, e2021GL093292 (2021).
199. Ogutu, G. E. O., Franssen, W. H. P., Supit, I., Omondi, P. & Hutjes, R. W. A. Skill of ECMWF system-4 ensemble seasonal climate forecasts for East Africa. *Int. J. Climatol.* **37**, 2734–2756 (2017).
200. Young, H. R. & Klingaman, N. P. Skill of seasonal rainfall and temperature forecasts for East Africa. *Weather. Forecast.* **35**, 1783–1800 (2020).
201. Funk, C. et al. Predicting East African spring droughts using Pacific and Indian Ocean sea surface temperature indices. *Hydrol. Earth Syst. Sci.* **18**, 4965–4978 (2014).
202. Mutai, C. C., Ward, M. N. & Colman, A. W. Towards the prediction of the East Africa short rains based on sea-surface temperature–atmosphere coupling. *Int. J. Climatol.* **18**, 975–997 (1998).
203. Nicholson, S. E. The predictability of rainfall over the greater Horn of Africa. Part I: prediction of seasonal rainfall. *J. Hydrometeorol.* **15**, 1011–1027 (2014).
204. Meehl, G. A. et al. Initialized earth system prediction from subseasonal to decadal timescales. *Nat. Rev. Earth Environ.* **2**, 340–357 (2021).
205. MacLeod, D. Seasonal forecasts of the East African long rains: insight from atmospheric relaxation experiments. *Clim. Dyn.* **53**, 4505–4520 (2019).
206. Phillips, H. E. et al. Progress in understanding of Indian Ocean circulation, variability, air–sea exchange, and impacts on biogeochemistry. *Ocean. Sci.* **17**, 1677–1751 (2021).
207. Majumdar, S. J. A review of targeted observations. *Bull. Am. Meteorol. Soc.* **97**, 2287–2303 (2016).
208. Dong, B., Haines, K. & Martin, M. Improved high resolution ocean reanalyses using a simple smoother algorithm. *J. Adv. Model. Earth Syst.* **13**, e2021MS002626 (2021).
209. Nordling, L. Scientists struggle to access Africa's historical climate data. *Nature* **574**, 605–606 (2019).
210. Smith, M. J. et al. Changing how Earth system modeling is done to provide more useful information for decision making, science, and society. *Bull. Am. Meteorol. Soc.* **95**, 1453–1464 (2014).
211. Webster, P. J. Meteorology: improve weather forecasts for the developing world. *Nature* **493**, 17–19 (2013).
212. Thomson, M. C., Muñoz, Á. G., Cousin, R. & Shumake-Guillemot, J. Climate drivers of vector-borne diseases in Africa and their relevance to control programmes. *Infect. Dis. Poverty* **7**, 81 (2018).
213. Mordecai, E. A., Ryan, S. J., Caldwell, J. M., Shah, M. M. & LaBeaud, A. D. Climate change could shift disease burden from malaria to arboviruses in Africa. *Lancet Planet. Heal.* **4**, e416–e423 (2020).
214. Allen, T. et al. Global hotspots and correlates of emerging zoonotic diseases. *Nat. Commun.* **8**, 1124 (2017).
215. Lipp, E. K., Huq, A. & Colwell, R. R. Effects of global climate on infectious disease: the cholera model. *Clin. Microbiol. Rev.* **15**, 757–770 (2002).
216. Tamerius, J. D. et al. Environmental predictors of seasonal influenza epidemics across temperate and tropical climates. *PLoS Pathog.* **9**, 1003194 (2013).
217. Palmer, P. I. et al. Net carbon emissions from African biosphere dominate pan-tropical atmospheric CO₂ signal. *Nat. Commun.* **10**, 3344 (2019).
218. Merbold, L. et al. Opportunities for an African greenhouse gas observation system. *Reg. Environ. Change* **21**, 104 (2021).
219. Wang, T. et al. Why is the Indo-Gangetic Plain the region with the largest NH₃ column in the globe during pre-monsoon and monsoon seasons? *Atmos. Chem. Phys.* **20**, 8727–8736 (2020).
220. Cai, W. et al. Projected response of the Indian Ocean Dipole to greenhouse warming. *Nat. Geosci.* **6**, 999–1007 (2013).
221. Tramberend, S. et al. Co-development of East African regional water scenarios for 2050. *One Earth* **4**, 434–447 (2021).
222. Zhao, G., Li, Y., Zhou, L. & Gao, H. Evaporative water loss of 1.42 million global lakes. *Nat. Commun.* **13**, 3686 (2022).
223. Haghghi, E., Madani, K. & Hoekstra, A. Y. The water footprint of water conservation using shade balls in California. *Nat. Sustain.* **1**, 358–360 (2018).
224. *Progress on Change in Water-Use Efficiency. Global Status and Acceleration Needs for SDG Indicator 6.4.1* (FAO and UN Water, 2021).
225. Acreman, M. C. et al. *Managed Flood Releases from Reservoirs: Issues and Guidance*. Report to DFID and World Commission on Dams, 86 (Centre for Ecology and Hydrology, 2000).
226. Wang, J. et al. Exploitation of drought tolerance-related genes for crop improvement. *Int. J. Mol. Sci.* **22**, 10265 (2021).
227. Biamah, E. K., Gichuki, F. N. & Kaumbutho, P. G. Tillage methods and soil and water conservation in eastern Africa. *Soil. Tillage Res.* **27**, 105–123 (1993).
228. Parncutt, R. The human cost of anthropogenic global warming: semi-quantitative prediction and the 1000-tonne rule. *Front. Psychol.* **10**, 2323 (2019).
229. Lehner, B. & Grill, G. Global river hydrography and network routing: baseline data and new approaches to study the world's large river systems. *Hydrol. Process.* **27**, 2171–2186 (2013).
230. Becker, A. et al. A description of the global land-surface precipitation data products of the Global Precipitation Climatology Centre with sample applications including centennial (trend) analysis from 1901–present. *Earth Syst. Sci. Data* **5**, 71–99 (2013).
231. Schneider, U. et al. GPCP's new land surface precipitation climatology based on quality-controlled in situ data and its role in quantifying the global water cycle. *Theor. Appl. Climatol.* **115**, 15–40 (2014).
232. Funk, C. et al. The climate hazards infrared precipitation with stations — a new environmental record for monitoring extremes. *Sci. Data* **2**, 150066 (2015).
233. Gedney, N., Huntingford, C., Comyn-Platt, E. & Wiltshire, A. Significant feedbacks of wetland methane release on climate change and the causes of their uncertainty. *Environ. Res. Lett.* **14**, 084027 (2019).
234. Schreck, C. J. & Semazzi, F. H. M. Variability of the recent climate of eastern Africa. *Int. J. Climatol.* **24**, 681–701 (2004).
235. Sutcliffe, J. & Parks, Y. *The Hydrology of the Nile* (IAHS, 1999).
236. Alsdorf, D. et al. Opportunities for hydrologic research in the Congo basin. *Rev. Geophys.* **54**, 378–409 (2016).
237. Sutcliffe, J. & Brown, E. Water losses from the Sudd. *Hydrol. Sci. J.* **63**, 527–541 (2018).

Acknowledgements

P.I.P., L.F., M.L. and R.P.A. acknowledge support from the UK National Centre for Earth Observation (NCEO) funded by the National Environment Research Council (NE/R016518/1). C.M.W. acknowledges funding of the Grantham Research Fellowship from the Grantham Foundation. K.G.W. acknowledges the Oxford Martin Programme on Transboundary Resource Management. M.G. acknowledges the Coproduction of Climate Services for East Africa project. B.D. and K.H. acknowledge support of the NCEO LTS-S and International Programme (NE/X006328/1). N.G. acknowledges support from the Newton Fund through the Met Office Climate Science for Service Partnership Brazil (CSSP Brazil).

Author contributions

P.I.P. originated the review and coordinated the writing. P.I.P., C.M.W., B.D., R.I.M., K.G.W., N.G., J.E.H., N.M. and S.S.F. led the writing of individual subsections, with contributions from R.P.A. C.M.W., B.D., R.I.M., N.G. and S.S.F. provided the figures. All authors helped to revise and refine earlier drafts.

Competing interests

The authors declare no competing interests.

Additional information

Supplementary information The online version contains supplementary material available at <https://doi.org/10.1038/s43017-023-00397-x>.

Peer review information *Nature Reviews Earth & Environment* thanks Victor Ongoma, David MacLeod and Lutz Merbold for their contribution to the peer review of this work.

Publisher's note Springer Nature remains neutral with regard to jurisdictional claims in published maps and institutional affiliations.

Springer Nature or its licensor (e.g. a society or other partner) holds exclusive rights to this article under a publishing agreement with the author(s) or other rightsholder(s); author self-archiving of the accepted manuscript version of this article is solely governed by the terms of such publishing agreement and applicable law.

© Springer Nature Limited 2023

¹School of GeoSciences, University of Edinburgh, Edinburgh, UK. ²National Centre for Earth Observation, University of Edinburgh, Edinburgh, UK. ³Grantham Institute, Imperial College London, London, UK. ⁴Department of Meteorology, University of Reading, Reading, UK. ⁵National Centre for Earth Observation, University of Reading, Reading, UK. ⁶The Environmental Change Institute, University of Oxford, Oxford, UK. ⁷Met Office Hadley Centre, Joint Centre for Hydrometeorological Research, Wallingford, UK. ⁸Center for Climate Systems Research, Columbia Climate School, Columbia University, New York, NY, USA. ⁹NASA Goddard Institute for Space Studies, New York, NY, USA. ¹⁰Joint Institute for Regional Earth System Science and Engineering, University of California Los Angeles, Los Angeles, CA, USA. ¹¹Jet Propulsion Laboratory, Pasadena, CA, USA. ¹²UK Centre for Ecology and Hydrology, Wallingford, UK. ¹³Department of Civil Engineering, University of Khartoum, Khartoum, Sudan. ¹⁴IGAD Climate Prediction and Applications Centre, Nairobi, Kenya. ¹⁵Kenya Meteorological Department, Nairobi, Kenya. ¹⁶Department of Atmospheric and Environmental Sciences, University at Albany, State University of New York (SUNY), Albany, NY, USA. ¹⁷Egyptian Meteorological Authority, Cairo, Egypt. ¹⁸Present address: School of Earth and Environmental Sciences, Cardiff University, Cardiff, UK.